DOE/ID/12079-50
ESL-64

DOE/ID/12079--50

DE82 019907

Electromagnetic Modeling of Three-Dimensional Bodies in Layered Earths Using Integral Equations

by

Philip E. Wannamaker and Gerald W. Hohmann

EARTH SCIENCE LABORATORY
UNIVERSITY OF UTAH RESEARCH INSTITUTE
420 Chipeta Way
Suite 120
Salt Lake City, Utah 84108

January 1982

Prepared for the
Department of Energy
Division of Geothermal Energy
Under Contract DE-AC07-80ID12079

DISCLAIMER

NOTICE

This report was prepared to document work sponsored by the United States Government. Neither the United States nor its agent, the United States Department of Energy, nor any Federal employees, nor any of their contractors, subcontractors or their employees, makes any warranty, express or implied, or assumes any legal liability or responsibility for the accuracy, completeness, or usefulness of any information, apparatus, product or process disclosed, or represents that its use would not infringe privately owned rights.

NOTICE

Reference to a company or product name does not imply approval or recommendation of the product by the University of Utah Research Institute or the U.S. Department of Energy to the exclusion of others that may be suitable.

TABLE OF CONTENTS

FIGURES

ABSTRACT

An algorithm based on the method of integral equations has been developed to simulate the electromagnetic response of 3-D bodies in layered earths. The inhomogeneities are replaced mathematically by an equivalent current distribution which is approximated by pulse basis functions. A matrix equation is constructed using the electric dyadic Green's function appropriate to a layered earth and is solved for the vector current in each cell. Subsequently, scattered fields are found by integrating electric and magnetic dyadic Green's functions over the scattering currents.

Efficient evaluation of the dyadic Green's functions is a major consideration in reducing computation time. We find that tabulation/interpolation of the six electric and five magnetic Hankel transforms defining the secondary Green's functions is preferable to any direct Hankel transform calculation using linear filters.

A comparison of responses over elongate 3-D bodies with responses over 2-D bodies of identical cross section using plane wave incident fields is the only check available on our solution. Agreement is excellent; however, the length that a 3-D body must have before departures between 2-D transverse electric and corresponding 3-D signatures are insignificant depends strongly on the layering. The 2-D transverse magnetic and corresponding 3-D calculations agree closely regardless of the layered host.

INTRODUCTION

Developments in computer and scale modeling over the past several years have contributed profoundly to our understanding of the relations between subsurface three-dimensional (3-D) resistivity structure and observed electromagnetic (EM) quantities. However, with a few exceptions (Lajoie and West, 1976; Meyer, 1977), EM simulations have been confined to inhomogeneities in half-spaces.

The importance of overburden layers in determining EM signatures over potential ore deposits has been recognized by mining geophysicists for some time. In addition, large-scale resistivity structures such as sedimentary basins or magma chambers, important in crust-mantle or geothermal investigations, may reside in an essentially one-dimensional regional host determined by the physiochemical conditions of the particular tectonic environment (Brace, 1971; Wannamaker et al., 1980).

To illuminate characteristics of EM scattering from bodies in layered earths, we have extended an existing integral equations algorithm previously used to model inhomogeneities in half spaces (Hohmann, 1975; Ting and Hohmann, 1981). Rather than detail responses of particular geological structures, which we intend to do in subsequent communication, we explore the theory and framework of the algorithm and verify its accuracy. A major issue which must be addressed is the derivation and efficient evaluation of the complicated electric and magnetic dyadic Green's functions, the kernels of the integral equations.

THEORY OF INTEGRAL EQUATIONS

Governing Equations

Consider a 3-D body in an n-layered host, shown confined to layer j for simplicity in Figure 1. The total electric and magnetic fields $(\vec{E}_t, \vec{H}_t)$ as a function of position $\bar{r}$ and for an $e^{i\omega t}$ time dependence obey Maxwell's equations

$$-\bar{\nabla}\times\vec{E}_t = \hat{z}\vec{H}_t + \vec{M}_i \qquad (1)$$

and

$$\bar{\nabla}\times\vec{H}_t = \vec{J}_t + \vec{J}_i \quad , \qquad (2)$$

where $\vec{J}_t = \hat{y}\vec{E}_t$ is the total current density, $\hat{y} = \sigma + i\omega\varepsilon$ is the admittivity and $\hat{z} = i\omega\mu$ is the impedivity at any point and where $\vec{J}_i$ and $\vec{M}_i$ are impressed electric and magnetic source currents. Conductivity, dielectric permittivity and magnetic permeability are σ, ε and μ.

In our solution, the 3-D body is replaced by an equivalent scattering current distribution (Harrington, 1961, p. 126). The total fields $(\vec{E}_t, \vec{H}_t)$ in any layer are hence decomposed into an incident set $(\vec{E}_i, \vec{H}_i)$, due to $\vec{J}_i$ and $\vec{M}_i$, and a scattered set $(\vec{E}_s, \vec{H}_s)$, contributed by the body. Helmholtz equations in layer l with the body in layer j can be written

$$(\bar{\nabla}^2 + k_l^2)\vec{E}_i = (\frac{-1}{\hat{y}_l}\bar{\nabla}\bar{\nabla}\cdot + \hat{z}_l)\vec{J}_i + \bar{\nabla}\times\vec{M}_i \quad , \qquad (3)$$

$$(\bar{\nabla}^2 + k_l^2)\vec{H}_i = (\frac{1}{\hat{z}_l}\bar{\nabla}\bar{\nabla}\cdot + \hat{y}_l)\vec{M}_i - \bar{\nabla}\times\vec{J}_i \quad , \qquad (4)$$

$$(\bar{\nabla}^2 + k_l^2)\vec{E}_s = 0 \qquad l\neq j \quad , \qquad (5)$$

$$(\bar{\nabla}^2 + k_l^2)\vec{H}_s = 0 \qquad l\neq j \quad , \qquad (6)$$

$$(\bar{\nabla}^2 + k_j^2)\vec{E}_s = (\frac{-1}{\hat{y}_j}\bar{\nabla}\bar{\nabla}\cdot + \hat{z}_j)\vec{J}_s + \bar{\nabla}\times\vec{M}_s \qquad l=j \qquad (7)$$

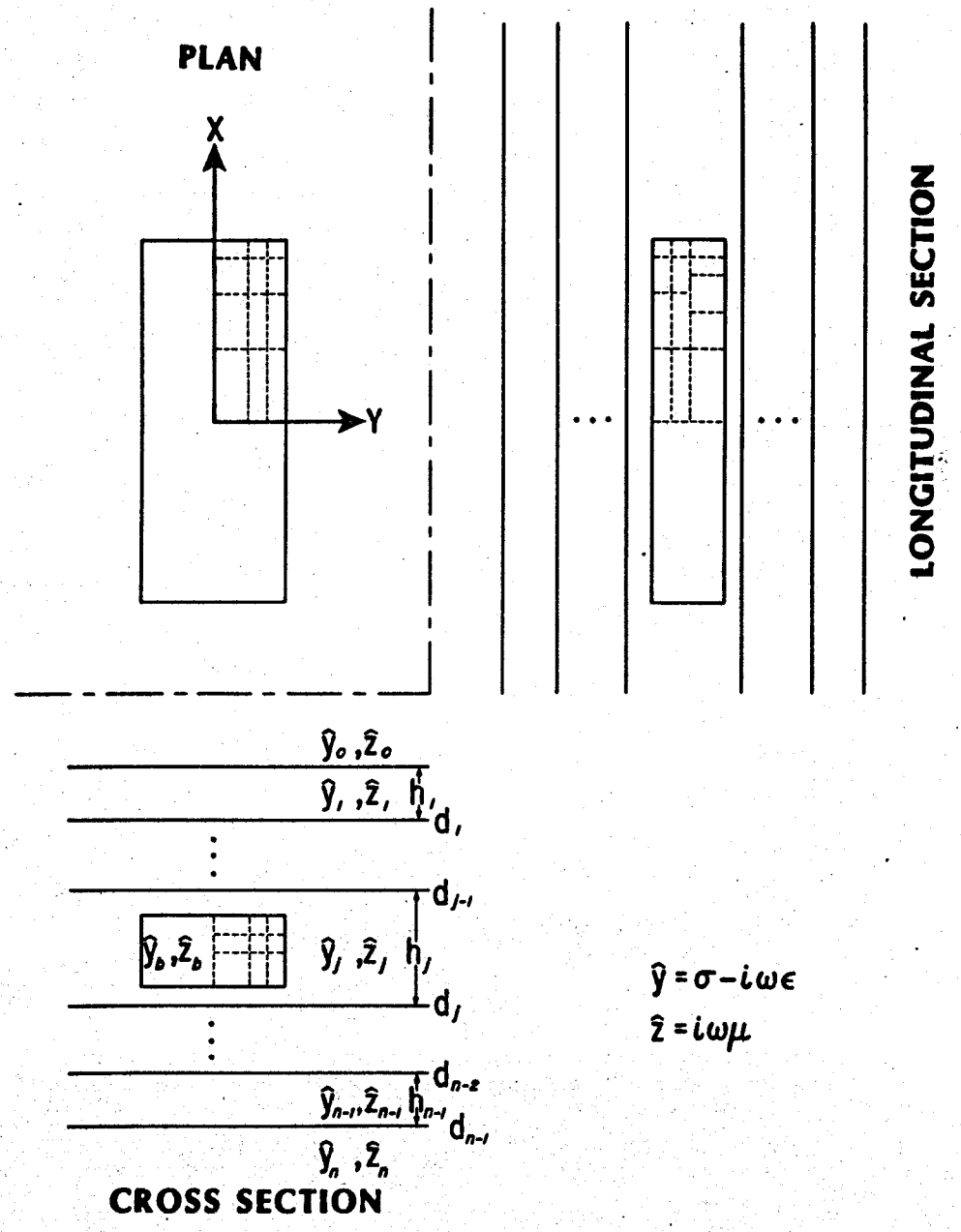

Figure 1. Principal views of 3-D prismatic body in an arbitrarily layered earth. Dashes outline a typical discretization of the body into rectangular cells, shown only for the right half of the body in section and upper right-hand quadrant in plan. The algorithm can treat bodies cutting across layer interfaces, although this is not shown in the figure.

and

$$(\bar{\nabla}^2 + k_j^2)\vec{H}_s = (\tfrac{1}{\hat{z}_j}\bar{\nabla}\bar{\nabla} + \hat{y}_j)\vec{M}_s - \bar{\nabla}\times\vec{J}_s \qquad l=j \quad , \quad (8)$$

in which $k_l = \sqrt{-\hat{z}_l\hat{y}_l}$ is the wavenumber in layer l. In (7) and (8), $\vec{J}_s = (\hat{y}_b - \hat{y}_j)\vec{E}_b$ and $\vec{M}_s = (\hat{z}_b - \hat{z}_j)\vec{H}_b$ are the equivalent scattering currents substituting for the body, while the total fields within the body, as yet unknown, are $\vec{E}_b$ and $\vec{H}_b$. When layer boundaries intersect the body, subscript j refers to any layer containing a portion of the body. Henceforth we assume that μ_l and μ_b equal the free space value μ_0 everywhere and drop $\vec{M}_s$ from consideration. Furthermore, displacement currents in the earth may be neglected, so that $\hat{y}_l = \sigma_l$ and $\hat{y}_b = \sigma_b$ hereafter.

The solutions to (5) through (8) are given by the integral equations

$$\vec{E}_s(\bar{r}) = \int_V \tilde{G}_l^E(\bar{r};\bar{r}')\cdot\vec{J}_s(\bar{r}')dv' \qquad (9)$$

and

$$\vec{H}_s(\bar{r}) = \int_V \tilde{G}_l^H(\bar{r};\bar{r}')\cdot\vec{J}_s(\bar{r}')dv' \quad , \quad (10)$$

valid for bodies cutting across layers. The quantities $\tilde{G}_l^E(\bar{r};\bar{r}')$ and $\tilde{G}_l^H(\bar{r};\bar{r}')$ are 3 x 3 dyadic Green's functions relating a vector field at $\bar{r}$ in layer l to a current element at $\bar{r}'$ in layer j, including $l = j$. These functions are derived in Appendix A.

Matrix Formation

Van Bladel (1961) has shown that (9) is valid even within the inhomogeneity, provided a suitable principal value for the integral is defined. A simple matrix solution can thus be found using the method of collocation with pulse subsectional basis functions (Harrington, 1968). The body is approximated by N rectangularly prismatic cells, each of dimensions $M_{xn}\Delta_n$ by $M_{yn}\Delta_n$ by $M_{zn}\Delta_n$, where M_{xn}, M_{yn} and M_{zn} are positive integers and Δ_n is the size of a cubic subcell in cell n (see Figures 1 and 2). Over each cell, the body conductivity σ_b and total electric field $\vec{E}_b$ are presumed constant. Rectangular cells are useful for approximating elongated inhomogeneities, since variations in $\vec{E}_b$ are more abrupt across shorter dimensions of the body than across longer ones.

Adding the solution of (3) to (9), the total electric field at the center of cell m due to all N cells is approximated by (Hohmann, 1975)

$$\vec{E}_b(\bar{r}_m) = \vec{E}_i(\bar{r}_m) + \sum_{n=1}^{N}(\sigma_{bn}-\sigma_j)\tilde{\Gamma}^E_i(\bar{r}_m;\bar{r}_n)\cdot\vec{E}_b(\bar{r}_n) \quad , \quad (11)$$

in which the electric dyadic Green's function for a rectangular prism of current is

$$\tilde{\Gamma}^E_i(\bar{r}_m;\bar{r}_n) = \int_{V_n}\tilde{G}^E_i(\bar{r}_m;\bar{r}')dv' \quad . \quad (12)$$

Rearranging (11) and using more concise notation,

$$\sum_{n=1}^{N}[(\sigma_{bn}-\sigma_j)\tilde{\Gamma}^E_{i(mn)} - \tilde{\delta}_{mn}]\cdot\vec{E}_{bn} = -\vec{E}_{im} \quad (13)$$

where

$$\tilde{\delta}_{mn} = \begin{cases} \tilde{I} & m = n \\ \tilde{0} & m \neq n \end{cases} \quad (14)$$

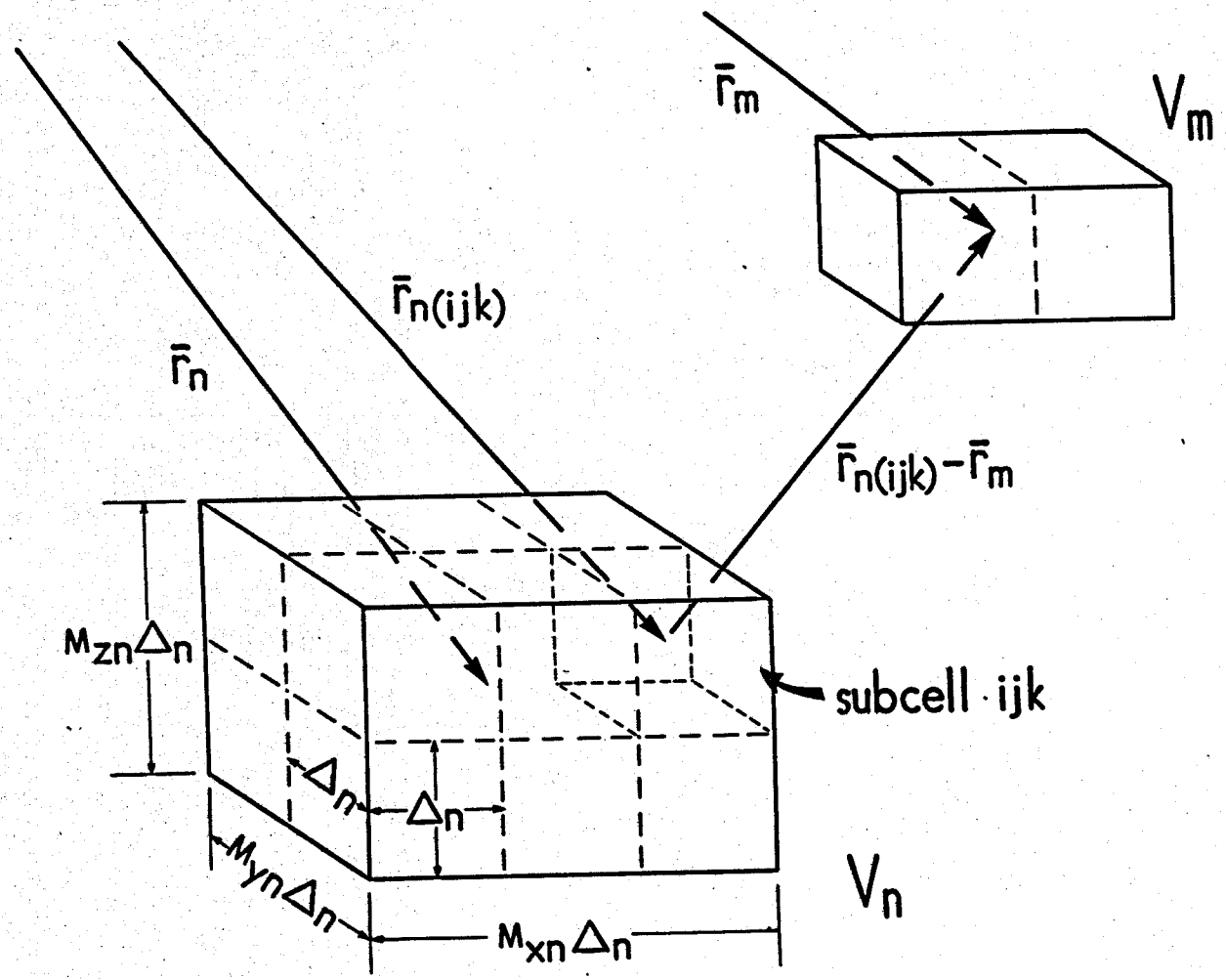

Figure 2. Geometric relation between rectangular cells m and n. As defined in equations (19) and (21), the electric field at the center of cell m at $\bar{r}_m$ is the sum of the fields due to each subcell comprising cell n at $\bar{r}_n$. The subcell position vector is $\bar{r}_{n(ijk)}$.

with $\tilde{I}$ and $\tilde{0}$ the 3 x 3 identity and null dyadics respectively. When written for all N values of m, (13) yields the matrix equation

$$[\mathcal{Z}]\cdot[\vec{E}_b] = [-\vec{E}_i] \tag{15}$$

to be solved for the electric fields within the cells. From these, scattered fields about the inhomogeneity are computed using discrete versions of (9) and (10), specifically

$$\vec{E}_s(\bar{r}) = \sum_{n=1}^{N}(\sigma_{bn}-\sigma_j)\tilde{\Gamma}_i^E(\bar{r};\bar{r}_n)\cdot\vec{E}_b(\bar{r}_n) \tag{16}$$

and

$$\vec{H}_s(\bar{r}) = \sum_{n=1}^{N}(\sigma_{bn}-\sigma_j)\tilde{\Gamma}_i^H(\bar{r};\bar{r}_n)\cdot\vec{E}_b(\bar{r}_n) \tag{17}$$

COMPUTATIONAL CONSIDERATIONS

Integration of Green's Functions

Calculation of $\tilde{\Gamma}^E_{\ell}(\bar{r}_m;\bar{r}_n)$ from $\tilde{G}^E_{\ell}(\bar{r};\bar{r}')$ for the matrix elements requires some care. When the inhomogeneity does not cut across layer interfaces, as in Figure 1, $\ell = j$ throughout in (13). Each cell in this case is coupled to every other cell by a Green's function composed of a primary or whole space component and a secondary component (see Appendix A), i.e.,

$$\tilde{\Gamma}^E_{\ell(mn)} = {}^P\tilde{\Gamma}^E_{\ell(mn)} + {}^S\tilde{\Gamma}^E_{\ell(mn)} \quad . \tag{18}$$

The primary component in turn is split into volume current and free charge contributions pertaining to the $\hat{z}_j\vec{J}_s$ and $\frac{1}{\gamma_j}\bar{\nabla}\bar{\nabla}\cdot\vec{J}_s$ terms in (7). The free charge contribution can be defined as the gradient of a scalar potential Ψ (Hohmann, 1975).

When computing matrix elements, a sufficient approximation for the volume integration is

$${}_V\Gamma^{P\tilde{E}}_{\ell(mn)} = \sum_{i=1}^{M_{xn}}\sum_{j=1}^{M_{yn}}\sum_{k=1}^{M_{zn}} {}_V\Gamma^{P\tilde{E}}_{\ell}(\bar{r}_m;\bar{r}_{n(ijk)}) \tag{19}$$

where ${}_V\Gamma^{P\tilde{E}}_{\ell}(\bar{r}_m;\bar{r}_{n(ijk)})$ is the volume Green's function for a cubic subcell of current as per Hohmann (1975). As defined in Figure 2, the subcell position vector is

$$\bar{r}_{n(ijk)} = \left(x_n + \Delta_n\left(\frac{M_{xn}+1}{2} - i\right)\right)\hat{i} + \left(y_n + \Delta_n\left(\frac{M_{yn}+1}{2} - j\right)\right)\hat{j} + \left(z_n + \Delta_n\left(\frac{M_{zn}+1}{2} - k\right)\right)\hat{k} \quad . \tag{20}$$

The charge term is similarly given as

$$ {}^{p}_{\gamma}\tilde{\Gamma}^{E}_{\ell(mn)} = \sum_{i=1}^{M_{xn}} \sum_{j=1}^{M_{yn}} \sum_{k=1}^{M_{zn}} {}^{p}_{\gamma}\tilde{\Gamma}^{E}_{\ell}(\bar{r}_m;\bar{r}_{n(ijk)}) \qquad (21) $$

but now ${}^{p}_{\gamma}\tilde{\Gamma}^{E}_{\ell}(\bar{r}_m;\bar{r}_{n(ijk)})$, the charge Green's function for a cubic subcell, is evaluated using the more involved integro-difference scheme adopted by Hohmann and Ting (1978). In calculating ${}^{s}\tilde{\Gamma}^{E}_{\ell(mn)}$ we do not specify charge and current terms, though they can be defined from (7). An integration analogous to (19) applies except that the cubic subcell is treated simply as a dipole current source, meaning

$$ {}^{s}\tilde{\Gamma}^{E}_{\ell}(\bar{r}_m;\bar{r}_{n(ijk)}) = \Delta_n^3 \, {}^{s}\tilde{G}^{E}_{\ell}(\bar{r}_m;\bar{r}_{n(ijk)}) \quad . \qquad (22) $$

If the body cuts across layer interfaces, subscripts ℓ and j in (13) refer to the layers containing cells m and n respectively. Cells in different layers are coupled only by secondary electric Green's functions, for which charge and current terms are not given. Added effort in determining $\tilde{\Gamma}^{E}_{\ell(mn)}$ is required since accurate analytic expressions like ${}^{p}_{\gamma}\tilde{\Gamma}^{E}_{\ell}(\bar{r}_m;\bar{r}_{n(ijk)})$ cannot be obtained. Whenever cells m and n are separated by an interface and $|\bar{r}_m-\bar{r}_{n(ijk)}| < \Delta_n$, a further division of the subcell into eight cubes, with each of these considered as in (22), is adequate.

The quantities $\tilde{\Gamma}^{E}_{\ell}(\bar{r};\bar{r}_n)$ and $\tilde{\Gamma}^{H}_{\ell}(\bar{r};\bar{r}_n)$ in (15) and (16) come about in a similar fashion. When the field point resides in the same layer as the cell, primary and secondary components to both electric and magnetic Green's functions again arise. Analogs to (19) and (21) are also employed in the integration, with the cubic subcells being treated as dipole sources as in (22) for all but the charge term. In this latter case, a surface integration over the cubic subcells in the manner of

Hohmann (1975) gives ${}^{P}_{\varphi}\tilde{\Gamma}^{E}_{z}(\bar{r};\bar{r}_{n(ijk)})$. We add that, since no charge appears within any rectangular cell, no scalar potential contributions to either matrix elements or scattered fields due to interior faces of the subcells need be computed in (21), thereby increasing the efficiency of the algorithm. When a receiver resides in a layer different from that of the cell considered, only secondary Green's functions exist, with the cubic subcells once more treated as dipoles.

Our method of integrating the dyadic Green's functions over the rectangular cells, for both matrix terms and scattered fields, is inherently more accurate than that of Das and Verma (1981), who replace such prisms by spheres and cylinders regardless of their aspect ratios.

Calculation of Green's Functions

Efficient evaluation of the dyadic Green's functions in Appendix A is necessary to avoid prohibitive computer time. The primary solutions are analytic expressions and present no problems, but the secondary Green's functions require Hankel transformation of complicated kernel functions.

To speed computation, tables of the six electric and five magnetic Hankel transforms are set up prior to matrix formation and scattered field calculation, from which specific values of ${}^{S}\tilde{G}^{E}_{z}(\bar{r};\bar{r}')$ and ${}^{S}\tilde{G}^{H}_{z}(\bar{r};\bar{r}')$ are obtained by cubic interpolation using Newton's Divided Difference method (Carnahan et al., 1969). For a given layered earth and frequency, the transforms are functions of horizontal distance (r), field point depth (z) and current depth (z'). Hence the matrix elements require a 3-D interpolating polynomial in r, z and z' whose formula is

$$
\begin{aligned}
f(r,z,z') = {} & f(r_1,z_1,z_1') + (r-r_1) f[r_2,r_1] + (z-z_1) f[z_2,z_1] + (z'-z_1') f[z_2',z_1'] \\
& + (r-r_1)(r-r_2) f[r_3,r_2,r_1] + (z-z_1)(z-z_2) f[z_3,z_2,z_1] + (z'-z_1')(z'-z_2') f[z_3',z_2',z_1'] \\
& + (r-r_1)(z-z_1) f[r_2,r_1;z_2,z_1] + (r-r_1)(z'-z_1') f[r_2,r_1;z_2',z_1'] + (z-z_1)(z'-z_1') f[z_2,z_1;z_2',z_1'] \\
& + (r-r_1)(r-r_2)(r-r_3) f[r_3,r_2,r_1,r_0] + (z-z_1)(z-z_2)(z-z_3) f[z_3,z_2,z_1,z_0] \\
& + (z'-z_1')(z'-z_2')(z'-z_3') f[z_3',z_2',z_1',z_0'] + (r-r_1)(r-r_2)(z-z_1) f[r_3,r_2,r_1;z_2,z_1] \\
& + (r-r_1)(z-z_1)(z-z_2) f[r_2,r_1;z_3,z_2,z_1] + (r-r_1)(r-r_2)(z'-z_1') f[r_3,r_2,r_1;z_2',z_1'] \\
& + (r-r_1)(z'-z_1')(z'-z_2') f[r_2,r_1;z_3',z_2',z_1'] + (z-z_1)(z-z_2)(z'-z_1') f[z_3,z_2,z_1;z_2',z_1'] \\
& + (z-z_1)(z'-z_1')(z'-z_2') f[z_2,z_1;z_3',z_2',z_1'] + (r-r_1)(z-z_1)(z'-z_1') f[r_2,r_1;z_2,z_1;z_2',z_1']
\end{aligned}
\tag{23}
$$

where a 3-D grid of basepoints r_i, z_i and z_i' is specified that is sufficient to cover all values of r, z and z' encountered for a given body. Various difference terms are defined by

$$
\begin{aligned}
f[r_2,r_1] &= [f(r_2,z_1,z_1') - f(r_1,z_1,z_1')]/(r_2-r_1) = f[r_2,r_1]\big|_{z_1,z_1'} \\
f[r_3,r_2,r_1] &= \{f[r_3,r_2]\big|_{z_1,z_1'} - f[r_2,r_1]\big|_{z_1,z_1'}\}/(r_3-r_1) = f[r_3,r_2,r_1]\big|_{z_1,z_1'} \\
f[r_3,r_2,r_1;z_2,z_1] &= \{f[r_3,r_2,r_1]\big|_{z_2,z_1'} - f[r_3,r_2,r_1]\big|_{z_1,z_1'}\}/(z_2-z_1) = f[r_3,r_2,r_1;z_2,z_1]\big|_{z_1'} \\
f[r_2,r_1;z_2,z_1;z_2',z_1'] &= \{f[r_2,r_1;z_2,z_1]\big|_{z_2'} - f[r_2,r_1;z_2,z_1]\big|_{z_1'}\}/(z_2'-z_1')
\end{aligned}
$$

etc. (Carnahan et al., 1969).

Field points generally reside on specified discrete levels of z (normally the surface at z = 0) and so the following 2-D formula in r and z' applies:

$$
\begin{aligned}
f(r,z') = {} & f(r_1,z_1') + (r-r_1) f[r_2,r_1] + (z'-z_1') f[z_2',z_1'] + (r-r_1)(r-r_2) f[r_3,r_2,r_1] \\
& + (z'-z_1')(z'-z_2') f[z_3',z_2',z_1'] + (r-r_1)(z'-z_1') f[r_2,r_1;z_2',z_1'] \\
& + (r-r_1)(r-r_2)(r-r_3) f[r_3,r_2,r_1,r_0] + (z'-z_1')(z'-z_2')(z'-z_3') f[z_3',z_2',z_1',z_0'] \\
& + (r-r_1)(r-r_2)(z'-z_1') f[r_3,r_2,r_1;z_2',z_1'] + (r-r_1)(z'-z_1')(z'-z_2') f[r_2,r_1;z_3',z_2',z_1']
\end{aligned}
\tag{24}
$$

A schematic of this interpolating polynomial appears in Figure 3.

New Hankel transform table values must be computed whenever layer parameters, frequency, body geometry or range of receiver distances are altered. These basepoint values are calculated using Anderson's (1975) subroutines ZHANK0 and ZHANK1. Note that exact function values are returned whenever 2-D or 3-D interpolating polynomials are evaluated at any of the basepoints. It therefore pays to select basepoints near cell and receiver locations if possible.

Computation Times

The cubic interpolating polynomials we use are certainly more time consuming than the linear interpolation of Hohmann (1975). However, several improvements in other aspects of the algorithm have resulted in computation times for construction and reduction of the matrix to be essentially those described by Ting and Hohmann (1981). Of the total run times for bodies consisting of more than about 40 cells, computation of the Hankel transform tables takes less than 2-3%.

Das and Verma (1981) suggest that direct use of a linear digital filtering technique such as that of Anderson (1975, 1979) is an efficient means of evaluating the Green's functions. We do not agree. Linear filter methods versatile enough to handle the wide range of layered earths of interest in electrical geophysics generally need in excess of 50 terms to evaluate a Hankel transform. Furthermore, the kernel values in each of these terms require time-consuming complex exponentiations, the number of which increases with the number of layers (see Appendix A). Our equations (21) and (22) have been programmed to require just 32 and 16 complex multiplications and additions to evaluate

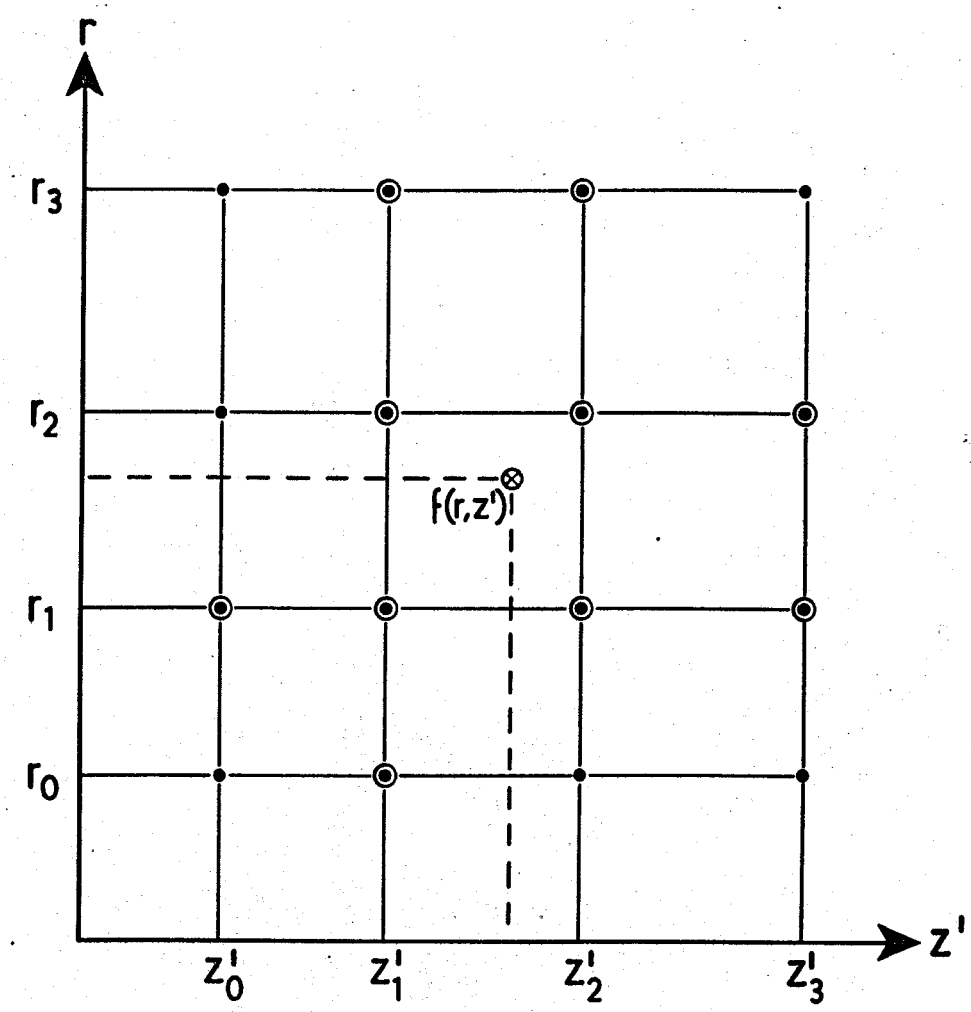

Figure 3. Distribution of basepoints around desired function for 2-D cubic interpolating polynomial. A 2-D grid of basepoints r_i and z_j is specified that is sufficient to cover all values of r and z' encountered for a given body and range of receiver distances.

a Hankel transform. Even so, the interpolations constitute the most time consuming part of the integrations. Thus, we believe that an algorithm such as ours, which employs tabulated transforms, will perform the necessary integrations for a given body-layering geometry in at least an order of magnitude less time than will a routine using linear filters throughout.

CHECKS ON THE SOLUTION

To this time, no one has published calculated responses of 3-D bodies in earths with layer interfaces both above and below the bodies, either for plane wave or finite sources. To establish the accuracy of our algorithm for this most general case, we can only compare computations for elongate 3-D bodies with those for 2-D structures of identical cross section using plane wave incident fields (see Appendix B).

Our program can accommodate an arbitrary number of layers but, for simplicity, we have considered an inhomogeneity in the upper layer of a two-layer earth (Figure 4). The body is a plate-like feature 1000 m thick at a depth of 750 m with the lower layer interface situated closely below at 2250 m. Its strike length is 40 km. Horizontal plate-like bodies within compact layer sequences demonstrate strongly the special effects of host layering on inhomogeneity responses. The intrinsic resistivity of the body is 5 Ω-m while that of the layer in which it resides is 200 Ω-m. Basement resistivities of 10, 200 and 4000 Ω-m were examined for plane wave excitation at 1.0 Hz.

Surface fields scattered from this 3-D body are compared with those from the corresponding 2-D structure, the latter calculated using a finite element routine (Rijo, 1977), in Figures 5, 6 and 7. The secondary electric field in the y-direction, E_{ys}, corresponds in the 2-D case to the transverse magnetic (TM mode) of excitation and has been normalized in the plots by the incident electric field magnitude at the earth's surface, $|E_{yo}|$. The transverse electric (TE) components E_{xs}, H_{ys} and H_{zs} have been normalized respectively by $|E_{xo}|$, $|H_{yo}|$ and $|H_{yo}|$.

Figure 4. Our solution is verified by comparing the response of this elongate 3-D body to the response of a 2-D body of identical cross section. Dashed lines show rectangular cell discretization with only half of the body shown in plan and longitudinal section. The smaller cells near the center give greater accuracy to the scattered fields along the y axis over the edge of the body. The strike length is 40 km, depth is 750 m, depth extent is 1000 m and width is 5 km.

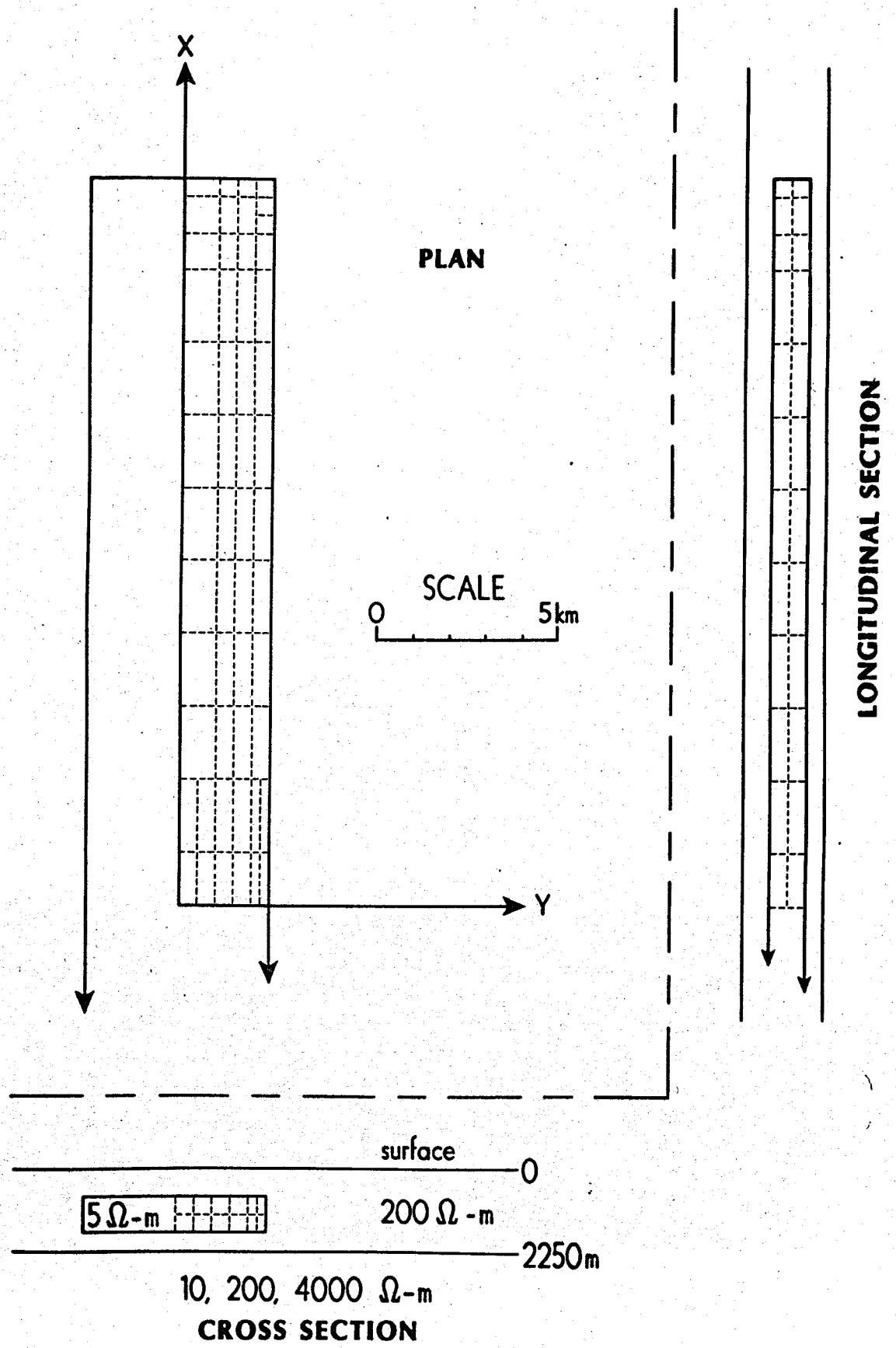
X
PLAN
SCALE
0
5km
Y
LONGITUDINAL SECTION
surface
0
5 Ω-m
200 Ω -m
2250m
10, 200, 4000 Ω-m
CROSS SECTION

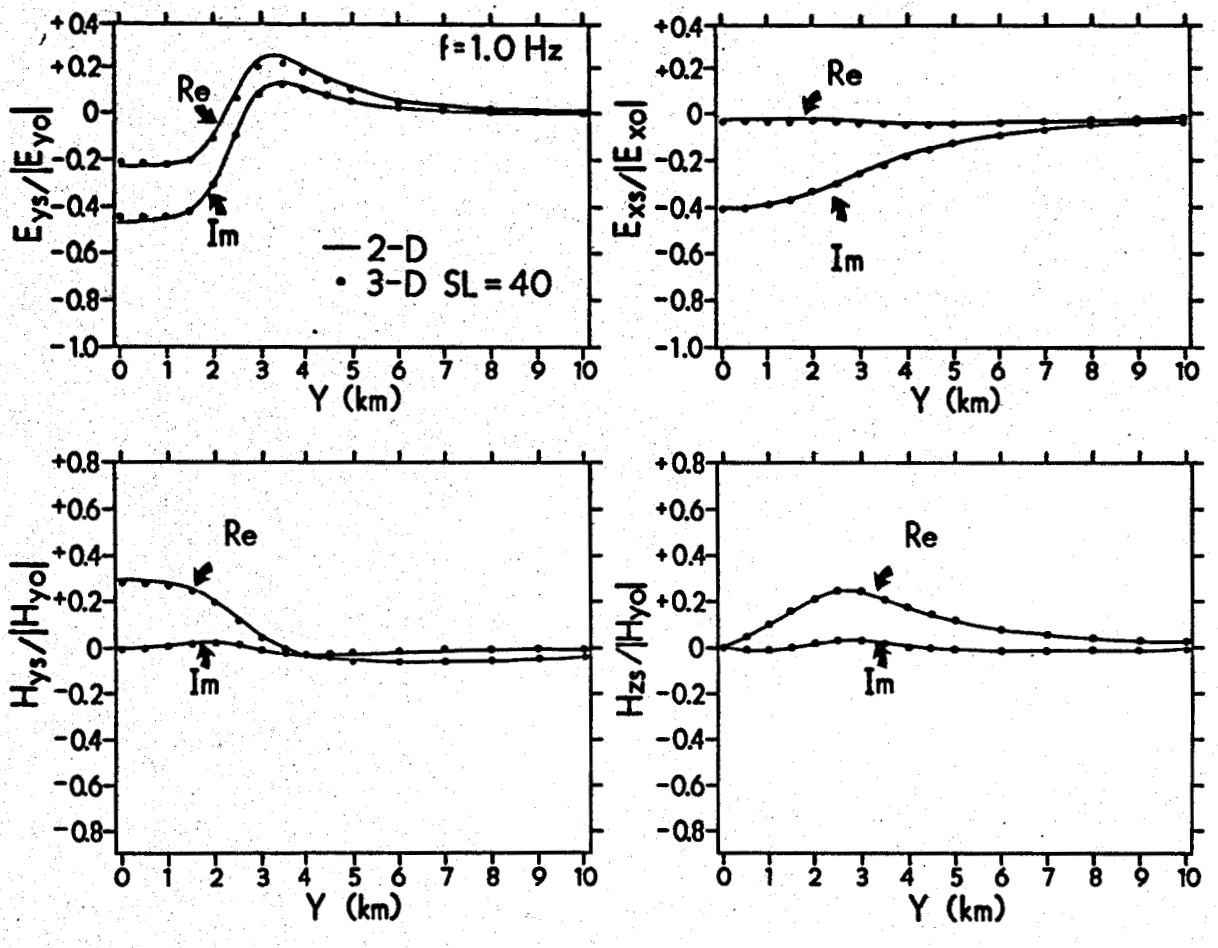

Figure 5. Profiles of normalized real (Re) and imaginary (Im) secondary electric and magnetic field components at 1.0 Hz along the y axis of the 3-D body of Figure 4 and across a 2-D body of identical cross section for a basement resistivity of 10. Ω-m. The response of the 3-D body, of strike length (SL) 40 km, is plotted using filled dots while that of the 2-D structure is shown as solid curves.

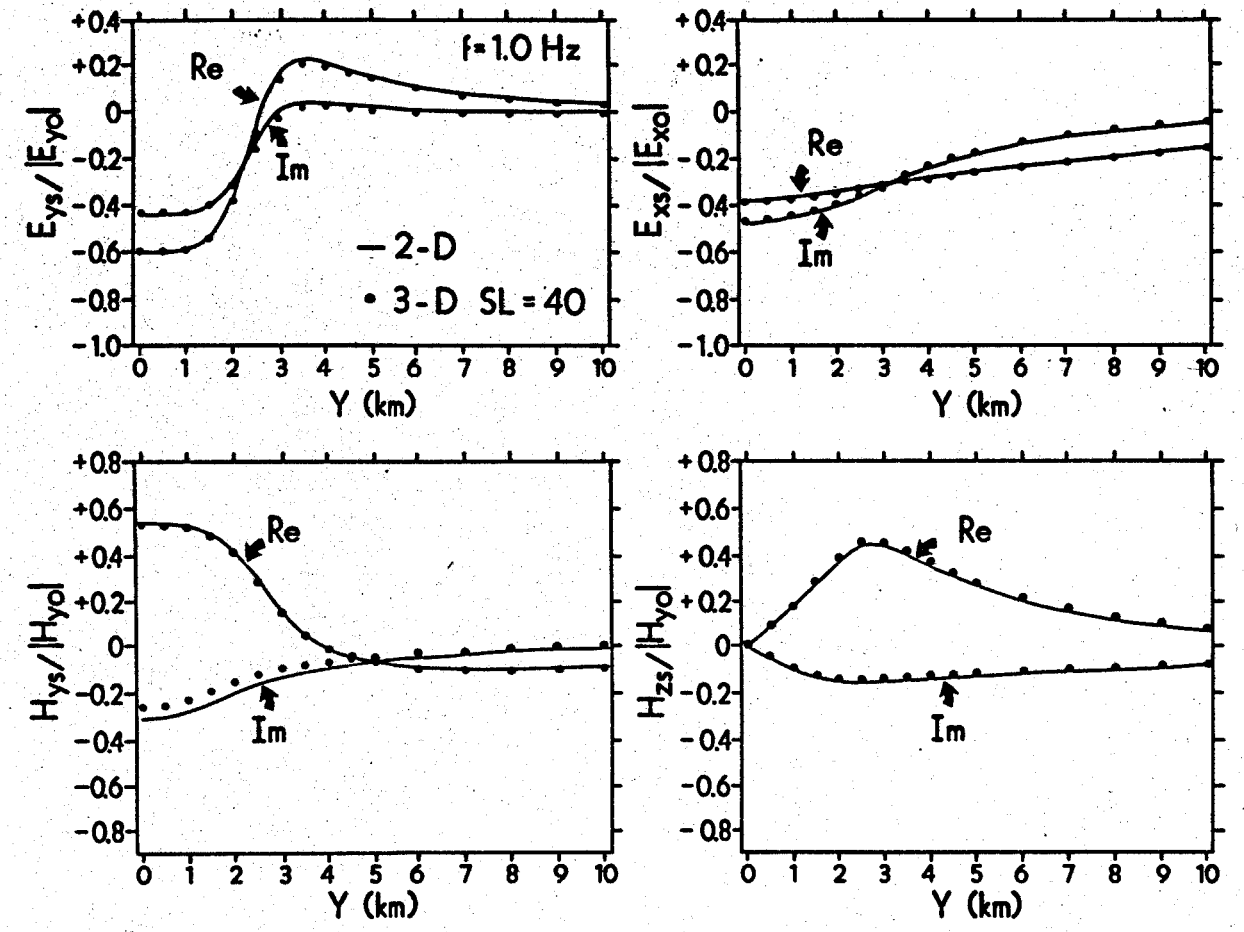

Figure 6. Profiles of normalized real (Re) and imaginary (Im) secondary electric and magnetic field components at 1.0 Hz along the y axis of the 3-D body of Figure 4 and across a 2-D body of identical cross section for a basement resistivity of 200. Ω-m. The response of the 3-D body, of strike length (SL) 40 km, is plotted using filled dots while that of the 2-D structure is shown as solid curves.

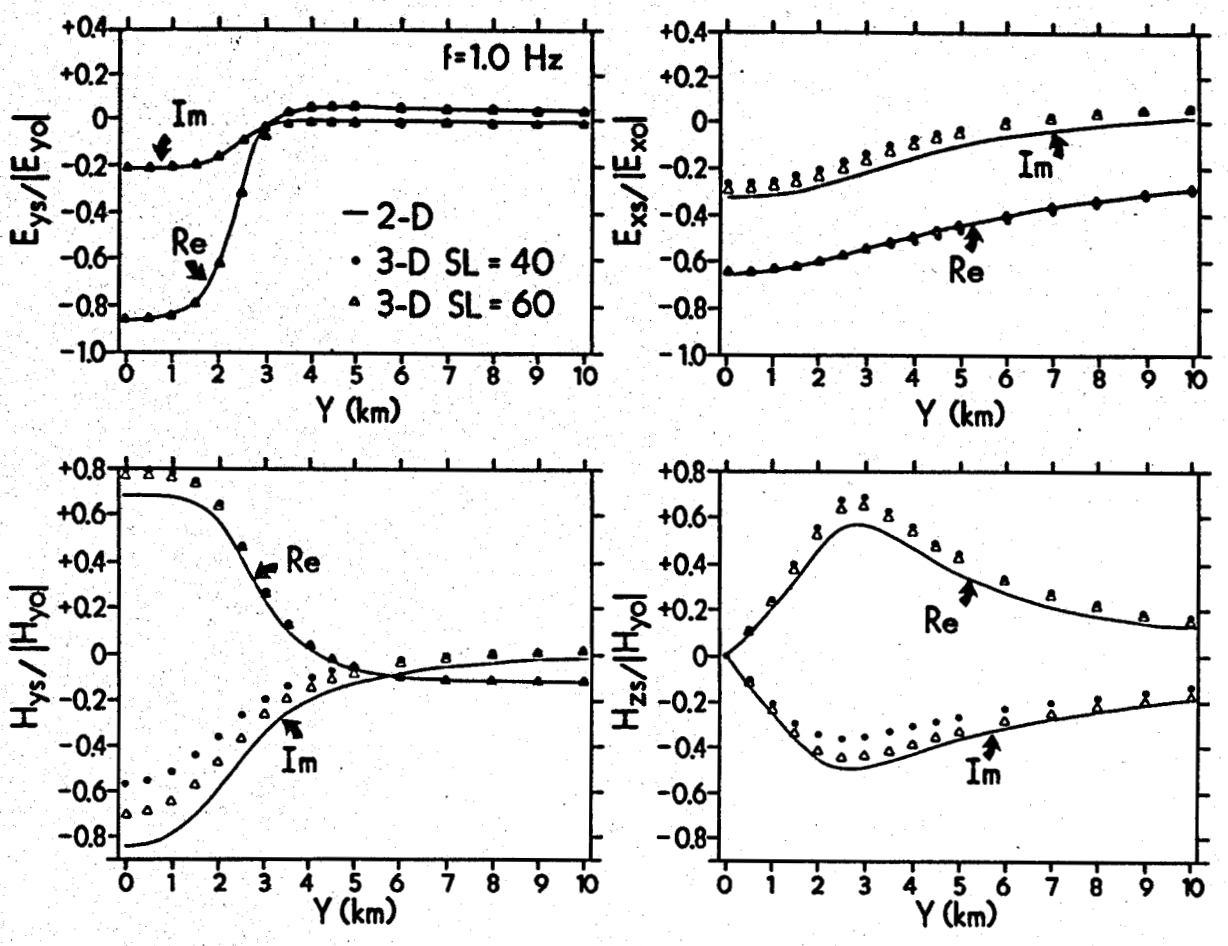

Figure 7. Profiles of normalized real (Re) and imaginary (Im) secondary electric and magnetic field components at 1.0 Hz along the y axis of the 3-D body of Figure 4, a similar 3-D body of SL = 60 km, and across a 2-D body of identical cross section for a basement resistivity of 4000. Ω-m. The response of the 60 km long 3-D body, plotted using open triangles, shows improved convergence over the response of the 40 km long body with the 2-D transverse electric results.

Agreement in Figure 5 between the 2-D and 3-D results for the 10 Ω-m basement is excellent, indicating that the 3-D body is sufficiently long at this frequency to appear two-dimensional and, more importantly, that our 3-D results are accurate. The same statement can be made regarding the results of Figure 6 where a 200 Ω-m basement was used, with the possible exception of the imaginary component of H_{ys}. In Figure 7 concerning the 4000 Ω-m basal half-space, however, a serious discrepancy is apparent between the 2-D TE calculations and those for the 40 km long 3-D structure. Evidently, the length that a 3-D body must be for it to behave two-dimensionally for the TE mode depends upon the 1-D sequence within which it resides.

By increasing the strike length of the 3-D body to 60 km, the agreement between 3-D and 2-D TE responses in Figure 7 is much improved. The lack of agreement between 3-D and 2-D responses when the resistive basement is considered is not due, for the most part, to any special features of the scattering currents within the body. The primary or whole-space electric Green's functions dominate the cell-to-cell coupling terms in the matrix $\mathcal{Z}$ of equation (14), so that the interior $\hat{E}$-field distributions using different layered hosts are largely scaled verions of each other with overall levels determined by $\hat{E}_i$. Indeed, this is the major reason for the peak amplitudes of H_{ys} and H_{zs} increasing in Figures 5 through 7 as the basement resistivity increases. For plane waves at a given frequency, resistive layer sequences result in larger values of $\hat{E}_i$, and hence $\hat{E}_b$ (but not $\hat{H}_i$), than do conductive ones.

It is instead the layered host containing a given 3-D body that determines whether 2-D and 3-D results agree. Two factors are at work here. First, dissipation of EM waves in resistive media is less than in conductive ones. Second, and we believe more importantly, current perturbations about a 3-D body overlying a resistive basement tend to be confined to the less resistive upper layer. This leads to a geometric attenuation of the secondary fields with distance that is slower when a resistive basement is present than when a conductive one is. In particular then, the contribution of free charge on the ends of the 3-D body to the secondary electric fields at the receiver points we have considered is stronger for a resistive basement than for a conductive one. Such free charge is not present on 2-D bodies for the TE mode. Similarly, the absence of scattering current beyond the ends of the 3-D structure (current which is present in the 2-D TE case) has an effect on the secondary $\vec{H}$-fields at the receivers considered that is greater when a resistive basement is present than when a conductive one is.

It is debatable whether the discrepancies remaining between the 3-D and 2-D TE calculations in Figure 7 seriously affect the magnetotelluric apparent resistivity and impedance phase, since these functions include the primary $\vec{E}$- and $\vec{H}$-fields in their definitions. However, the 10-15% differences in the secondary H-field components would translate to commensurate departures between 3-D and 2-D Tipper estimates, which we do not find satisfactory.

The 2-D TM and 3-D E_y profiles agree closely, regardless of the layered host, since free charge on the boundaries of the body is included implicitly in both these formulations. The lack of charge and

scattering current beyond the ends of the 3-D body, charge and current which are present in the 2-D TM case do not contribute materially to its secondary $\hat{E}$-fields. A very small component of H_{xs} exists for the 3-D body, which is zero for the 2-D TM mode, but its magnitude is less than 3% of $|H_{xo}|$ for the resistive basement, and even smaller for the other basements, and does not affect in any important manner the apparent resistivity or impedance phase. These functions are overwhelmingly dominated by $\hat{E}$-field variations.

CONCLUSIONS

An algorithm based on integral equations is an accurate and flexible means of simulating EM responses of 3-D bodies in layered earths. The calculations we have shown, in addition to verifying our numerical solution, indicate that body responses may be strongly influenced by the nature of the layering. Future communication by our research group will pursue this matter for geological structures of economic and academic interest for both plane wave and finite sources.

Integration of the dyadic Green's functions for the matrix elements and the scattered fields is the most time-consuming part of our routine. We have found that tabulation and interpolation of the many requisite Hankel transforms provide a much more efficient means of computing the Green's functions than does a direct transform evaluation using linear filters or any other method.

Pulse basis functions are a definite limitation on modeling very shallow or complex 3-D resistivity distributions. Before these latter problems become tractable, modeling techniques requiring far fewer unknowns than ours must be developed, such as hybrid finite element-integral equations concepts (Petrick et al., 1981; Lee et al., 1981). We believe, however, that our method will be very valuable in EM survey design, in recognizing fundamental 3-D effects and in demonstrating the applicability of 1-D and 2-D approaches in 3-D environments.

ACKNOWLEDGEMENTS

We are grateful to Drs. Stanley H. Ward and William R. Sill for reviewing the manuscript and to William R. Petrick, William S. San Filipo and Gregory H. Steemson for many valuable discussions. W. San Filipo was also responsible for developing the capability to discretize the body into rectangular cells. In addition, we thank Terry J. Killpack and Carleen Nutter for much guidance on use of the PRIME 400 computer, upon which the algorithm was run.

This research was supported by DOE/DGE contract DE-AC07-80ID12079.

REFERENCES

Anderson, W.L., 1975, Improved digital filters for evaluating Fourier and Hankel transform integrals: U.S.G.S. rept. USGS-GD-75-012; avail. as NTIS rept. PB-242-800/1WC, 223 p.

Anderson, W. L., 1979, Numerical integration of related Hankel transforms of orders 0 and 1 by adaptive digital filtering: Geophysics, 44(7), p. 1287-1305.

Banos, A., Jr., 1966, Dipole radiation in the presence of a conducting half-space: Pergamon Press, New York, 208 p.

Brace, W. F., 1971, Resistivity of saturated crustal rocks to 40 km based on laboratory measurements, In J. G. Heacock (ed.) The Structure and Physical Properties of the Earth's Crust, American Geophysical Union Mono. 14, p. 243-256.

Carnahan, B., Luther, H.A., and Wilkes, J.O., 1969, Applied numerical methods: John Wiley & Sons, New York, 604 p.

Das, U.C. and Verma, S.K., 1981, Numerical considerations on computing the EM response of three-dimensional inhomogeneities in a layered earth: Geop. J. Royal Ast. Soc., 66, p. 733-740.

Erdelyi, A., 1954, Tables of integral transforms, v. 2: McGraw-Hill Book Co., New York, 451 p.

Gradshteyn, I.S. and Ryzhik, I.M., 1980, Table of integrals, series and products: Academic Press, New York, 1160 p.

Harrington, R.F., 1961, Time-harmonic electromagnetic fields: McGraw-Hill Electrical and Electronic Engineering Series, McGraw-Hill Book Co., New York, 480 p.

Harrington, R.F., 1968, Field computation by moment methods: MacMillan Co., New York, 229 p.

Hohmann, G.W., 1975, Three-dimensional induced polarization and electromagnetic modeling: Geophysics, 40(2), p. 309-324.

Hohmann, G.W. and Ting, S.C., 1978, Three-dimensional magnetotelluric modeling: Earth Science Lab. rept. 7, Salt Lake City, 48 p.

Lajoie, J.J. and West, G.F., 1976, The electromagnetic response of a conductive inhomogeneity in a layered earth: Geophysics, 41(6A), p. 1133-1156.

Lee, K.H., Pridmore, D.F. and Morrison, H.F., 1981, A hybrid three-dimensional electromagnetic modeling scheme: Geophysics, 46(5), p. 796-805.

Meyer, W.H., 1977, Computer modeling of electromagnetic prospecting methods: Ph.D. thesis, Univ. of California at Berkeley, 155 p.

Petrick, W.R., Ward, S.H. and Hohmann, G.W., 1981, Three-dimensional electromagnetic modeling using a hybrid technique; abstract of paper presented at 50th annual meeting of the SEG, Houston: Geophysics, 46(4), p. 468.

Rijo, L., 1977, Modeling of electric and electromagnetic data: Ph.D. thesis, Univ. of Utah.

Stoyer, C.H., 1977, Electromagnetic fields of dipoles in stratified media: IEEE Trans. of Antennas and Propagation, AP-25, p. 547-552.

Tang, C.M., 1979, Electromagnetic fields due to dipole antennas embedded in stratified anistropic media: IEEE Trans. on Antennas and Propagation, AP-27, p. 665-670.

Ting, S.C. and Hohmann, G.W., 1981, Integral equation modeling of three-dimensional magnetotelluric response: Geophysics, 46(2), p. 182-197.

Van Bladel, J., 1961, Some remarks on Green's dyadic for infinite space: IRE Trans. on Antennas and Propagation, 9, p. 563-566.

Wait, J.R., 1970, Electromagnetic waves in stratified media: Pergamon Press, New York, 372 p.

Wannamaker, P.E., Ward, S.H., Hohmann, G.W. and Sill, W.R., 1980, Magnetotelluric models of the Roosevelt Hot Springs thermal area, Utah: Univ. of Utah Topical rept. DOE/ET/27002-8, 213 p.

Ward, S.H., 1967, Electromagnetic theory for geophysical application, In Mining Geophysics, v. II: SEG, Tulsa, p. 10-196.

Weidelt, P., 1975, Electromagnetic induction in three-dimensional structures: Geop. J. Royal Ast. Soc., 41, p. 85-109.

APPENDIX A

DYADIC GREEN'S FUNCTIONS FOR AN AC ELECTRIC DIPOLE IN A LAYERED CONDUCTING EARTH

Electric and magnetic fields at any point (x,y,z) in layer ℓ are related to a current element $\vec{J}dv'$ at (x',y',z') in layer j (see Figure A-1), where

$$\vec{J}dv' = J_x dv'\hat{i} + J_y dv'\hat{j} + J_z dv'\hat{k} \quad , \quad \text{(A-1)}$$

by 3 x 3 dyadic Green's functions through

$$\vec{E}_\ell(\bar{r}) = \tilde{G}^E_\ell(\bar{r};\bar{r}')\cdot\vec{J}(\bar{r}')dv' \quad \text{(A-2a)}$$

and

$$\vec{H}_\ell(\bar{r}) = \tilde{G}^H_\ell(\bar{r};\bar{r}')\cdot\vec{J}(\bar{r}')dv' \quad . \quad \text{(A-2b)}$$

Fields about a dipole in a layered earth have been been published by Weidelt (1975) and Stoyer (1977) using Hertz potentials and by Tang (1979) using a TE-TM formulation. However, for the sake of others who may wish to use our work, it is important that our Green's functions be specified in detail. Care was taken to define the functions in forms amenable to computation.

Our derivation employs the Schelkunoff vector potentials $\vec{A}$ and $\vec{F}$, which is possible since $\bar{\nabla}\cdot\vec{E}_\ell = \bar{\nabla}\cdot\vec{H}_\ell = 0$ for all ℓ except at the source (Harrington, 1961, p. 129-132). These potentials obey the wave equations

$$(\bar{\nabla}^2 + k_\ell^2)\vec{A}_\ell = \vec{J} \quad \text{(A-3a)}$$

and

$$(\bar{\nabla}^2 + k_\ell^2)\vec{F}_\ell = \vec{M} \quad , \quad \text{(A-3b)}$$

with $\vec{J}$ and $\vec{M}$ being volume distributions of electric and magnetic current. Note with this definition that our source in (A-1), to be

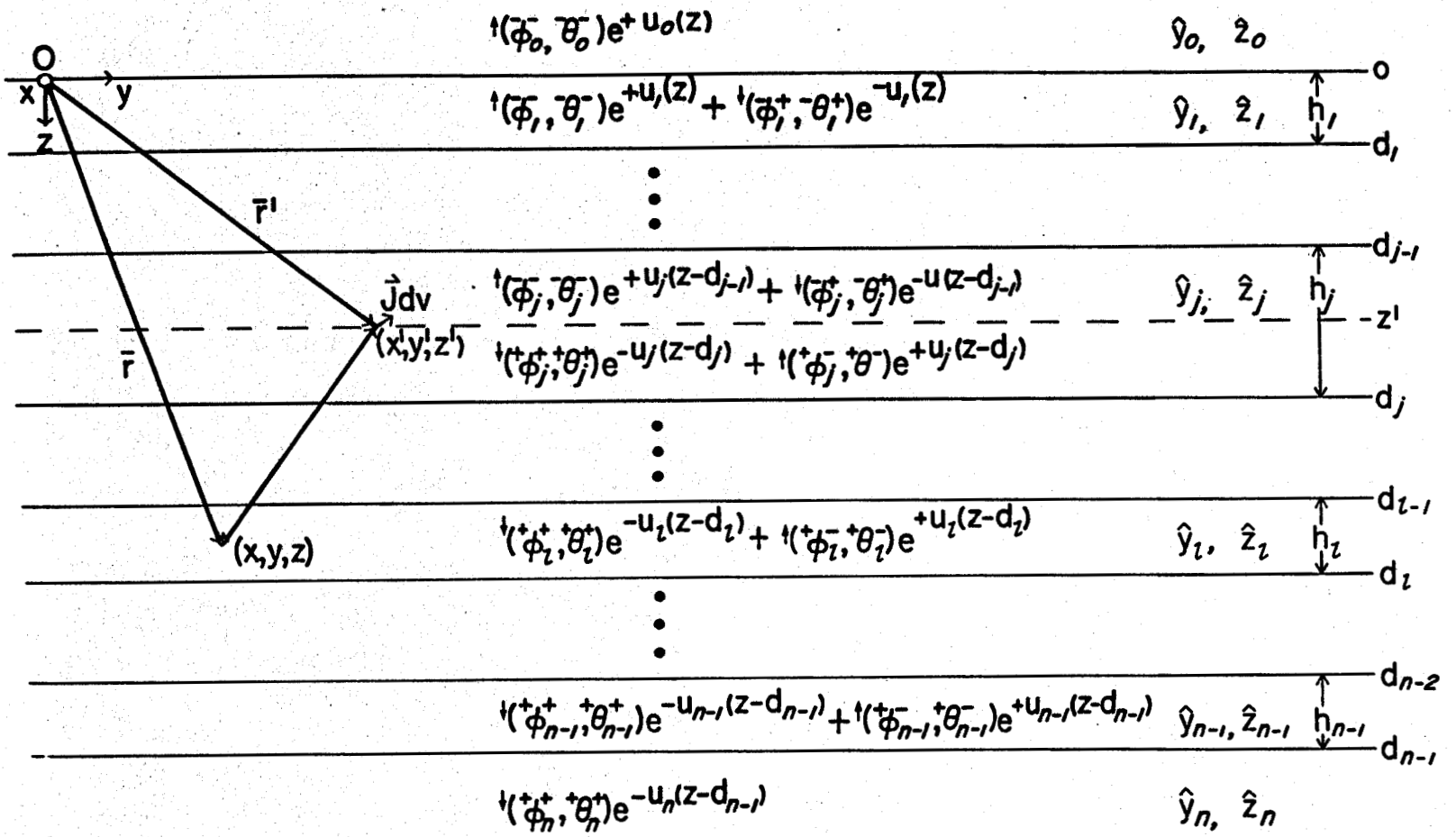

Figure A-1. Geometric relation between electric current element $\vec{J}dv'$ at (x',y',z') in layer j to field point at (x,y,z) in layer l. Also shown are general solutions to Debye potentials ϕ and θ in each medium, with upward and downward pointing arrows denoting direction of propagation.

considered a volume distribution, would be written as $\vec{J} = \vec{J}dv'\delta(\bar{r}-\bar{r}')$ for use in (A-3a), with $\delta(\bar{r}-\bar{r}')$ the Kronecker delta function. The fields may be obtained in each layer through

$$\vec{E}_l = -\bar{\nabla}\times\vec{F}_l - \hat{z}_l\vec{A}_l + \frac{1}{\hat{\gamma}_l}\bar{\nabla}\bar{\nabla}\cdot\vec{A}_l \qquad \text{(A-4a)}$$

and

$$\vec{H}_l = \bar{\nabla}\times\vec{A}_l - \hat{\gamma}_l\vec{F}_l + \frac{1}{\hat{z}_l}\bar{\nabla}\bar{\nabla}\cdot\vec{F}_l \quad . \qquad \text{(A-4b)}$$

Following Harrington, we express our current source $\vec{J}dv'$ in terms of an equivalent distribution of vertically oriented electric and magnetic sources. This reduces our task to determining only vertical components of $\vec{A}_l$ (hereafter designated ϕ_l) and $\vec{F}_l$ (designated θ_l) which obey the scalar wave equations

$$(\bar{\nabla}^2 + k_l^2)\phi_l = J_z^{eq} \qquad \text{(A-5a)}$$

and

$$(\bar{\nabla}^2 + k_l^2)\theta_l = M_z^{eq} \quad , \qquad \text{(A-5b)}$$

with J_z^{eq} and M_z^{eq} being the equivalent vertical source distributions. Equation (A-4) in cartesian coordinates becomes

$$E_{xl} = \frac{1}{\hat{\gamma}_l}\frac{\partial^2\phi_l}{\partial x\partial z} - \frac{\partial\theta_l}{\partial y} \quad , \qquad H_{xl} = \frac{\partial\phi_l}{\partial y} + \frac{1}{\hat{z}_l}\frac{\partial^2\theta_l}{\partial x\partial z} \quad , \qquad \text{(A-6a)}$$

$$E_{yl} = \frac{1}{\hat{\gamma}_l}\frac{\partial^2\phi_l}{\partial y\partial z} + \frac{\partial\theta_l}{\partial x} \quad , \qquad H_{yl} = \frac{-\partial\phi_l}{\partial x} + \frac{1}{\hat{z}_l}\frac{\partial^2\theta_l}{\partial y\partial z} \quad , \qquad \text{(A-6b)}$$

$$E_{zl} = \frac{1}{\hat{\gamma}_l}\left(\frac{\partial^2}{\partial z^2} + k_l^2\right)\phi_l \qquad \text{and} \qquad H_{zl} = \frac{1}{\hat{z}_l}\left(\frac{\partial^2}{\partial z^2} + k_l^2\right)\theta_l \quad . \qquad \text{(A-6c)}$$

Observe that E_{zl} is formulated solely in terms of ϕ_l while H_{zl} is solely in terms of θ_l. This choice of potentials has thus separated the fields into modes transverse magnetic (TM) and transverse electric (TE) to z.

Using the two-dimensional spatial Fourier transform pair,

$$f(x,y,z) = \frac{1}{4\pi^2} \iint_{-\infty}^{\infty} F(k_x,k_y,z)\, e^{+i(k_x x + k_y y)}\, dk_x dk_y \qquad \text{(A-7a)}$$

and

$$F(k_x,k_y,z) = \iint_{-\infty}^{\infty} f(x,y,z)\, e^{-i(k_x x + k_y y)}\, dx\, dy \quad , \qquad \text{(A-7b)}$$

the solutions to equation (A-5) in (k_x, k_y) space are given as upward and downward propagating plane waves in each homogeneous region of the form

$$\bar{\phi}_l = \bar{\phi}_l^- e^{+u_l(z-d_{l-1})} + \bar{\phi}_l^+ e^{-u_l(z-d_{l-1})} \qquad \text{(A-8a)}$$

and

$$\bar{\theta}_l = \bar{\theta}_l^- e^{+u_l(z-d_{l-1})} + \bar{\theta}_l^+ e^{-u_l(z-d_{l-1})} \quad , \qquad \text{(A-8b)}$$

for $z < z'$, and

$$^{+}\phi_l = {}^{+}\phi_l^- e^{+u_l(z-d_l)} + {}^{+}\phi_l^+ e^{-u_l(z-d_l)} \qquad \text{(A-9a)}$$

and

$$^{+}\theta_l = {}^{+}\theta_l^- e^{+u_l(z-d_l)} + {}^{+}\theta_l^+ e^{-u_l(z-d_l)} \quad , \qquad \text{(A-9b)}$$

for $z > z'$. The righthand + and - superscripts refer to downward and upward waves (see Figure A-1) and $u_l^2 = k_x^2 + k_y^2 - k_l^2$. Relation (A-6) is now

$$E_{xl} = \frac{ik_x}{\hat{\gamma}_l} \frac{\partial \phi_l}{\partial z} - ik_y \theta_l \quad , \qquad H_{xl} = ik_y \phi_l + \frac{ik_x}{\hat{z}_l} \frac{\partial \theta_l}{\partial z} \quad , \qquad \text{(A-10a)}$$

$$E_{yl} = \frac{ik_y}{\hat{\gamma}_l} \frac{\partial \phi_l}{\partial z} + ik_x \theta_l \quad , \qquad H_{yl} = -ik_x \phi_l + \frac{ik_y}{\hat{z}_l} \frac{\partial \theta_l}{\partial z} \quad , \qquad \text{(A-10b)}$$

$$E_{zl} = \frac{(k_x^2 + k_y^2)}{\hat{\gamma}_l} \phi_l \qquad \text{and} \qquad H_{zl} = \frac{(k_x^2 + k_y^2)}{\hat{z}_l} \theta_l \quad . \qquad \text{(A-10c)}$$

The general solutions (A-8) and (A-9) are constructed as the sum of primary or particular solutions, which appear only in region j containing the source, plus source-free secondary or complementary solutions, which appear everywhere and are chosen to satisfy boundary conditions (Harrington, 1961, p. 129-132). The primary solutions ${}^{P}\phi_j$ and ${}^{P}\theta_j$ result by equating relation (A-10c) to the vertical components of electric and magnetic fields for current components J_x and J_z in a whole space of wavenumber k_j^*. These fields in turn are obtained by applying equation (A-4) to the whole space potentials (Harrington, 1961, p. 78)

$$ {}^{P}A_{xj} = \frac{J_x dv'}{4\pi} \frac{e^{-ik_j[(x-x')^2 + (y-y')^2 + (z-z')^2]^{1/2}}}{[(x-x')^2 + (y-y')^2 + (z-z')^2]^{1/2}} \qquad \text{(A-11a)} $$

and

$$ {}^{P}A_{zj} = \frac{J_z dv'}{4\pi} \frac{e^{-ik_j[(x-x')^2 + (y-y')^2 + (z-z')^2]^{1/2}}}{[(x-x')^2 + (y-y')^2 + (z-z')^2]^{1/2}} \quad , \qquad \text{(A-11b)} $$

which in (k_x,k_y) space are (Erdelyi, 1954, v. 2, p. 9)

$$ {}^{P}A_{xj} = \frac{J_x}{2u_j} e^{-i(k_x x' + k_y y')} e^{-u_j|z-z'|} \qquad \text{(A-12a)} $$

and

$$ {}^{P}A_{zj} = \frac{J_z}{2u_j} e^{-i(k_x x' + k_y y')} e^{-u_j|z-z'|} \quad . \qquad \text{(A-12b)} $$

For J_x, the fields from a Fourier transformed version of (A-4) are

$$ {}^{P}E^{x}_{zj} = \frac{ik_x}{\hat{\gamma}_j} \frac{\partial {}^{P}A_{xj}}{\partial z} = \pm \frac{J_x ik_x}{2\hat{\gamma}_j} e^{-i(k_x x' + k_y y')} e^{-u_j|z-z'|} \qquad \text{(A-13a)} $$

* We drop consideration of J_y for now. Green's function elements for this component are derived by analogy with those for J_x and are simply stated at the end of this analysis.

and

$$ {}^{p}H^{x}_{zj} = -ik_y {}^{p}A_{xj} = -\frac{J_x ik_y}{2u_j} e^{-i(k_x x' + k_y y')} e^{-u_j|z-z'|} \quad , \qquad \text{(A-13b)} $$

where ± applies above/below the current element. For J_z, we find

$$ {}^{p}E^{z}_{zj} = \frac{(k_x^2 + k_y^2)}{\hat{y}_j} {}^{p}A_{zj} = \frac{J_z(k_x^2 + k_y^2)}{2\hat{y}_j u_j} e^{-i(k_x x' + k_y y')} e^{-u_j|z-z'|} \qquad \text{(A-14a)} $$

and

$$ {}^{p}H^{z}_{zj} = 0 \quad . \qquad \text{(A-14b)} $$

Equating (A-10c) with (A-13), we have for an x-directed current element

$$ {}^{p}\phi^{x}_{j} = \pm \frac{J_x ik_x}{2(k_x^2 + k_y^2)} e^{-i(k_x x' + k_y y')} e^{-u_j|z-z'|} \qquad \text{(A-15a)} $$

and

$$ {}^{p}\theta^{x}_{j} = -\frac{J_x \hat{z}_j ik_y}{2u_j(k_x^2 + k_y^2)} e^{-i(k_x x' + k_y y')} e^{-u_j|z-z'|} \quad . \qquad \text{(A-15b)} $$

Equating (A-10c) with (A-14), we have for a z-directed current element

$$ {}^{p}\phi^{z}_{j} = \frac{J_z}{2u_j} e^{-i(k_x x' + k_y y')} e^{-u_j|z-z'|} \qquad \text{(A-16a)} $$

and

$$ {}^{p}\theta^{z}_{j} = 0 \quad . \qquad \text{(A-16b)} $$

Comparing (A-15) and (A-16) with (A-12), the equivalent electric and magnetic source distributions in terms of the original dipole are seen to be

$$ J_z^{eq}(k_x, k_y) = \pm \frac{J_x u_j ik_x}{(k_x^2 + k_y^2)} + J_z \qquad \text{(A-17a)} $$

and

$$M_z^{eq}(k_x,k_y) = -\frac{J_x \hat{z}_j \imath k_y}{(k_x^2 + k_y^2)} \quad . \quad \text{(A-17b)}$$

The equivalent sources are not discrete current elements at (x',y',z') but are distributed over the x-y plane at z = z'.

The upward and downward waves of equation (A-8) in any layer above the dipole are related through reflection coefficients $^{-}R_i^{TM}$ and $^{-}R_i^{TE}$ by

$$^{-}\phi_i^{+} = {}^{-}R_i^{TM}\, {}^{-}\phi_i^{-} \quad \text{(A-18a)}$$

and

$$^{-}\theta_i^{+} = {}^{-}R_i^{TE}\, {}^{-}\theta_i^{-} \quad . \quad \text{(A-18b)}$$

After Wait (1970), the reflection coefficients are

$$^{-}R_i^{TM} = \frac{Z_i - {}^{-}\bar{Z}_i}{Z_i + {}^{-}\bar{Z}_i} \quad \text{(A-19a)}$$

and

$$^{-}R_i^{TE} = \frac{Y_i - {}^{-}\bar{Y}_i}{Y_i + {}^{-}\bar{Y}_i} \quad , \quad \text{(A-19b)}$$

with the following recurrence relations

$$^{-}\bar{Z}_i = Z_i \frac{{}^{-}\bar{Z}_{i-1} + Z_i \tanh(u_i h_i)}{Z_i + {}^{-}\bar{Z}_{i-1} \tanh(u_i h_i)} \quad \text{(A-20a)}$$

and

$$^{-}\bar{Y}_i = Y_i \frac{{}^{-}\bar{Y}_{i-1} + Y_i \tanh(u_i h_i)}{Y_i + {}^{-}\bar{Y}_{i-1} \tanh(u_i h_i)} \quad , \quad \text{(A-20b)}$$

where $Z_i = \frac{u_i}{\sigma_i}$, $Y_i = \frac{u_i}{\imath \omega_i}$ and $h_i = d_i - d_{i-1}$. Hence (A-8) in region j becomes

$$^{-}\phi_j = {}^{-}\phi_j^{-} \left[e^{+u_j(z-d_{j-1})} + {}^{-}R_j^{TM}\, e^{-u_j(z-d_{j-1})} \right] \quad \text{(A-21a)}$$

and

$$^{-}\theta_j = {}^{-}\theta_j^{-}\left[e^{+u_j(z-d_{j-1})} + {}^{-}R_j^{TE}\, e^{-u_j(z-d_{j-1})}\right] \qquad \text{(A-21b)}$$

Similarly, equation (A-9) in layer j becomes, for $z > z'$,

$$^{+}\phi_j = {}^{+}\phi_j^{+}\left[{}^{+}R_j^{TM} e^{+u_j(z-d_j)} + e^{-u_j(z-d_j)}\right] \qquad \text{(A-22a)}$$

and

$$^{+}\theta_j = {}^{+}\theta_j^{+}\left[{}^{+}R_j^{TE} e^{+u_j(z-d_j)} + e^{-u_j(z-d_j)}\right] \qquad \text{(A-22b)}$$

The reflection coefficients here, and for any other layer below the dipole, are

$$^{+}R_i^{TM} = \frac{Z_i - {}^{+}\bar{Z}_i}{Z_i + {}^{+}\bar{Z}_i} \qquad \text{(A-23a)}$$

and

$$^{+}R_i^{TE} = \frac{Y_i - {}^{+}\bar{Y}_i}{Y_i + {}^{+}\bar{Y}_i} \qquad \text{(A-23b)}$$

with

$$^{+}\bar{Z}_i = Z_i \frac{{}^{+}\bar{Z}_{i+1} + Z_i \tanh(u_i h_i)}{Z_i + {}^{+}\bar{Z}_{i+1}\tanh(u_i h_i)} \qquad \text{(A-24a)}$$

and

$$^{+}\bar{Y}_i = Y_i \frac{{}^{+}\bar{Y}_{i+1} + Y_i \tanh(u_i h_i)}{Y_i + {}^{+}\bar{Y}_{i+1}\tanh(u_i h_i)} \qquad \text{(A-24b)}$$

Unlike a dipole beneath overburden (Lee et al., 1981), $^{-}\phi_j$ and $^{-}\theta_j$ in (A-21) are not identified with only the primary potentials. Instead, they are the sum of the primary plus secondary upward reflected potentials due to the layering beneath the dipole. We write

$$^{-}\phi_j = \left[{}^{P}\phi_j^{-} + {}^{S}\phi_j^{-}\right]\left[e^{+u_j(z-d_{j-1})} + {}^{-}R_j^{TM}\, e^{-u_j(z-d_{j-1})}\right] \qquad \text{(A-25a)}$$

and

$$^{-}\theta_j = [^{p}\bar{\theta}_j^{-} + {}^{s}\theta_j^{-}][e^{+u_j(z-d_{j-1})} + {}^{-}R_j^{TE} e^{-u_j(z-d_{j-1})}] \quad . \qquad \text{(A-25b)}$$

Below the source, however, the primary potentials are downgoing, and the total potentials here in layer j can be written

$$^{+}\phi_j^{+} = {}^{s}\phi_j^{-} e^{+u_j(z-d_{j-1})} + {}^{p+}\phi_j^{+} e^{-u_j(z-d_{j-1})} + {}^{p-}\phi_j^{-} {}^{-}R_j^{TM} e^{-u_j(z-d_{j-1})} + {}^{s}\phi_j^{-} {}^{-}R_j^{TM} e^{-u_j(z-d_{j-1})} \qquad \text{(A-26a)}$$

and

$$^{+}\theta_j^{+} = {}^{s}\theta_j^{-} e^{+u_j(z-d_{j-1})} + {}^{p+}\theta_j^{+} e^{-u_j(z-d_{j-1})} + {}^{p-}\theta_j^{-} {}^{-}R_j^{TE} e^{-u_j(z-d_{j-1})} + {}^{s}\theta_j^{-} {}^{-}R_j^{TE} e^{-u_j(z-d_{j-1})} \quad , \qquad \text{(A-26b)}$$

which must equal equation (A-22). In this latter relation, $^{+}\phi_j^{+} {}^{+}R_j^{TM} e^{+u_j(z-d_j)}$ and $^{+}\theta_j^{+} {}^{+}R_j^{TE} e^{+u_j(z-d_j)}$ represent only secondary upward reflections due to the basal layering so, with (A-26), we find

$$^{+}\phi_j^{+} {}^{+}R_j^{TM} = {}^{s}\phi_j^{-} e^{+u_j h_j} \qquad \text{(A-27a)}$$

and

$$^{+}\theta_j^{+} {}^{+}R_j^{TE} = {}^{s}\theta_j^{-} e^{+u_j h_j} \quad . \qquad \text{(A-27b)}$$

Thus, one may equate ϕ_j^{+} and θ_j^{+} terms in (A-22) and (A-26) to get

$${}^{s}\phi_j^{-} = \frac{[{}^{p+}\phi_j^{+} + {}^{p-}\phi_j^{-} {}^{-}R_j^{TM}] {}^{+}R_j^{TM} e^{-2u_j h_j}}{1 - {}^{+}R_j^{TM} {}^{-}R_j^{TM} e^{-2u_j h_j}} \qquad \text{(A-28a)}$$

and

$${}^{s}\theta_j^{-} = \frac{[{}^{p+}\theta_j^{+} + {}^{p-}\theta_j^{-} {}^{-}R_j^{TE}] {}^{+}R_j^{TE} e^{-2u_j h_j}}{1 - {}^{+}R_j^{TE} {}^{-}R_j^{TE} e^{-2u_j h_j}} \quad . \qquad \text{(A-28b)}$$

The relation between $^{p+}\phi_j^{+}$ and $^{p-}\phi_j^{-}$ and between $^{p+}\theta_j^{+}$ and $^{p-}\theta_j^{-}$ depends upon whether one considers J_x or J_z as the source. For J_x alone, from equation (A-15),

$${}^{p-}\phi_j^{-x} = -e^{-2u_j(z'-d_{j-1})} {}^{p+}\phi_j^{+x} \qquad \text{(A-29a)}$$

and

$$ {}^{P-}\theta_j^{-x} = e^{-2u_j(z'-d_{j-1})}\,{}^{P+}\theta_j^{+x} \quad , \qquad \text{(A-29b)} $$

where

$$ {}^{P+}\phi_j^{+x} = \frac{-s_x\, i k_x}{(k_x^2+k_y^2)}\, e^{+u_j(z'-d_{j-1})} \qquad \text{(A-30a)} $$

and

$$ {}^{P+}\theta_j^{+x} = \frac{-s_x\, \hat{z}_j\, i k_y}{u_j(k_x^2+k_y^2)}\, e^{+u_j(z'-d_{j-1})} \quad . \qquad \text{(A-30b)} $$

For conciseness we have set $s_x = \frac{1}{2} J_x\, e^{-i(k_x x' + k_y y')}$. For J_z only, from (A-16), there results

$$ {}^{P-}\phi_j^{-z} = e^{-2u_j(z'-d_{j-1})}\,{}^{P+}\phi_j^{+z} \qquad \text{(A-31)} $$

with

$$ {}^{P+}\phi_j^{+z} = \frac{s_z}{u_j}\, e^{+u_j(z'-d_{j-1})} \qquad \text{(A-32)} $$

and where $s_z = \frac{1}{2} J_z\, e^{-i(k_x x' + k_y y')}$. Finally, with (A-22), (A-23), (A-28), (A-29) and (A-30), one obtains for an x-component of current density alone

$$ \phi_j^x = \frac{s_x\, i k_x}{(k_x^2+k_y^2)} \left\{ \left[\pm e^{-u_j|z-z'|} + {}^{-}R_j^{TM} e^{-u_j(z+z'-2d_{j-1})} \right] + {}^{x}A_j^{TM} \left[e^{+u_j(z-d_{j-1})} + {}^{-}R_j^{TM} e^{-u_j(z-d_{j-1})} \right] \right\} \qquad \text{(A-33a)} $$

and

$$ \theta_j^x = \frac{-s_x\, \hat{z}_j\, i k_y}{u_j(k_x^2+k_y^2)} \left\{ \left[e^{-u_j|z-z'|} + {}^{-}R_j^{TE} e^{-u_j(z+z'-2d_{j-1})} \right] + {}^{x}A_j^{TE} \left[e^{+u_j(z-d_{j-1})} + {}^{-}R_j^{TE} e^{-u_j(z-d_{j-1})} \right] \right\} . \qquad \text{(A-33b)} $$

With (A-22), (A-23), (A-28), (A-31) and (A-32), one obtains for J_z alone

$$ \phi_j^z = \frac{s_z}{u_j} \left\{ \left[e^{-u_j|z-z'|} + {}^{-}R_j^{TM} e^{-u_j(z+z'-2d_{j-1})} \right] + {}^{z}A_j^{TM} \left[e^{+u_j(z-d_{j-1})} + {}^{-}R_j^{TM} e^{-u_j(z-d_{j-1})} \right] \right\} \quad . \qquad \text{(A-34)} $$

We have also defined

$$ {}^{x}A_j^{TM} = \frac{{}^{+}R_j^{TM} e^{-2u_j h_j} e^{+u_j(z'-d_{j-1})}\left[{}^{-}R_j^{TM} e^{-2u_j(z'-d_{j-1})} - 1\right]}{1 - {}^{+}R_j^{TM}\,{}^{-}R_j^{TM} e^{-2u_j h_j}} \qquad \text{(A-35a)} $$

$$ {}^{x}A_j^{TE} = \frac{{}^{+}R_j^{TE} e^{-2u_j h_j} e^{+u_j(z'-d_{j-1})}\left[{}^{-}R_j^{TE} e^{-2u_j(z'-d_{j-1})} + 1\right]}{1 - {}^{+}R_j^{TE}\,{}^{-}R_j^{TE} e^{-2u_j h_j}} \qquad \text{(A-35b)} $$

and

$$ {}^{z}A_j^{TM} = \frac{{}^{+}R_j^{TM} e^{-2u_j h_j} e^{+u_j(z'-d_{j-1})}\left[{}^{-}R_j^{TM} e^{-2u_j(z'-d_{j-1})} + 1\right]}{1 - {}^{+}R_j^{TM}\,{}^{-}R_j^{TM} e^{-2u_j h_j}} \qquad \text{(A-35c)} $$

Continuity of tangential electric and magnetic fields across interfaces, along with (A-21) and (A-22), yields the potentials in other layers. For layer $\ell > j$, we obtain

$$ {}^{+}\phi_\ell^{+} = \prod_{m=j+1}^{\ell} \frac{\left[1 + {}^{+}R_{m-1}^{TM}\right] e^{-u_m h_m}}{\left[1 + {}^{+}R_m^{TM} e^{-2u_m h_m}\right]}\; {}^{+}\phi_j^{+} = {}^{+}B_{\ell j}^{TM}\; {}^{+}\phi_j^{+} \qquad \text{(A-37a)} $$

and

$$ {}^{+}\theta_\ell^{+} = \prod_{m=j+1}^{\ell} \frac{\left[1 + {}^{+}R_{m-1}^{TE}\right] e^{-u_m h_m}}{\left[1 + {}^{+}R_m^{TE} e^{-2u_m h_m}\right]}\; {}^{+}\theta_j^{+} = {}^{+}B_{\ell j}^{TE}\; {}^{+}\theta_j^{+} \qquad \text{(A-37b)} $$

Specification of the solution for $\ell = n$ is given later with the Green's functions. Combining (A-33) and (A-37), we get for J_x

$$ \phi_\ell^{x} = \frac{s_x i k_x}{(k_x^2 + k_y^2)}\left[{}^{+}B_{\ell j}^{TM}\left({}^{x}A_j^{TM} e^{+u_j h_j} / {}^{+}R_j^{TM}\right)\right]\left[{}^{+}R_\ell^{TM} e^{+u_\ell(z-d_\ell)} + e^{-u_\ell(z-d_\ell)}\right] \qquad \text{(A-38a)} $$

and

$$ \theta_\ell^{x} = \frac{-s_x \hat{z}_j i k_y}{u_j(k_x^2 + k_y^2)}\left[{}^{+}B_{\ell j}^{TE}\left({}^{x}A_j^{TE} e^{+u_j h_j} / {}^{+}R_j^{TE}\right)\right]\left[{}^{+}R_\ell^{TE} e^{+u_\ell(z-d_\ell)} + e^{-u_\ell(z-d_\ell)}\right] \qquad \text{(A-38b)} $$

Combining (A-34) and (A-37), for J_z and $\ell > j$ we have

$$ \phi_\ell^{z} = \frac{s_z}{u_j}\left[{}^{+}B_{\ell j}^{TM}\left({}^{z}A_j^{TM} e^{+u_j h_j} / {}^{+}R_j^{TM}\right)\right]\left[{}^{+}R_\ell^{TM} e^{+u_\ell(z-d_\ell)} + e^{-u_\ell(z-d_\ell)}\right] \qquad \text{(A-39)} $$

For layer $\ell < j$ above the current element, we have

$$\bar{\phi}_\ell = \prod_{m=j-1}^{\ell} \frac{[1+\bar{R}^{TM}_{m+1}]e^{-u_m h_m}}{[1+\bar{R}^{TM}_m e^{-2u_m h_m}]} \; \bar{\phi}_j = \bar{B}^{TM}_{\ell j} \; \bar{\phi}_j \qquad \text{(A-40a)}$$

and

$$\bar{\theta}_\ell = \prod_{m=j-1}^{\ell} \frac{[1+\bar{R}^{TE}_{m+1}]e^{-u_m h_m}}{[1+\bar{R}^{TE}_m e^{-2u_m h_m}]} \; \bar{\theta}_j = \bar{B}^{TE}_{\ell j} \; \bar{\theta}_j \qquad \text{(A-40b)}$$

Specification when $\ell = 0$ is also given later with the Green's functions. Combining (A-33) and (A-40), we get for J_x

$$\phi^x_\ell = \frac{s_x i k_x}{(k_x^2+k_y^2)} [\bar{B}^{TM}_{\ell j}(e^{-u_j(z'-d_{j-1})} + {}^xA^{TM}_j)][e^{+u_\ell(z-d_{\ell-1})} + \bar{R}^{TM}_\ell e^{-u_\ell(z-d_{\ell-1})}] \qquad \text{(A-41a)}$$

and

$$\theta^x_\ell = \frac{-s_x \hat{z}_j i k_y}{u_j(k_x^2+k_y^2)} [\bar{B}^{TE}_{\ell j}(e^{-u_j(z'-d_{j-1})} + {}^xA^{TE}_j)][e^{+u_\ell(z-d_{\ell-1})} + \bar{R}^{TE}_\ell e^{-u_\ell(z-d_{\ell-1})}] \qquad \text{(A-41b)}$$

Finally, with (A-34) and (A-40), for J_z and $\ell < j$ we have

$$\phi^z_\ell = \frac{s_z}{u_j} [{}^+B^{TM}_{\ell j}(e^{-u_j(z'-d_{j-1})} + {}^zA^{TM}_j)][e^{+u_\ell(z-d_{\ell-1})} + \bar{R}^{TM}_\ell e^{-u_\ell(z-d_{\ell-1})}] \qquad \text{(A-42)}$$

The Green's function elements in (k_x,k_y) space are obtained by substituting equations (A-33), (A-34), (A-38), (A-39), (A-41) and (A-42) in turn into relation (A-10) and setting the amplitude of each component of $\vec{J}dv'$ equal to unity. The results in cartesian coordinates will then come about by application of (A-7b). Omitting all that algebra, we proceed directly to a Hankel transform definition of the elements, which is necessary for our computation. This requires (Banos, 1966)

$$\iint_{-\infty}^{\infty} F(k_x^2+k_y^2) e^{i(k_x x + k_y y)} dk_x dk_y = 2\pi \int_0^\infty F(\lambda) \lambda J_o(\lambda r) d\lambda \qquad \text{(A-43)}$$

where $\lambda^2 = k_x^2 + k_y^2$, $r^2 = (x-x')^2 + (y-y')^2$ and $J_0(\lambda r)$ is the zeroth order Bessel function of the first kind. We will furthermore need the relations

$$\frac{\partial}{\partial x} \overset{F.T.}{\Longleftrightarrow} ik_x \qquad \frac{\partial}{\partial y} \overset{F.T.}{\Longleftrightarrow} ik_y \quad , \tag{A-44}$$

where F.T. denotes Fourier Transformation, and

$$\frac{\partial}{\partial z}\left(\frac{e^{-u_j|z-z'|}}{u_j}\right) = \pm e^{-u_j|z-z'|} \quad . \tag{A-45}$$

In addition we must use (Erdelyi, 1954, v. 2, p. 9)

$$\int_0^\infty \frac{e^{-u_j|z-z'|}}{u_j} \lambda J_0(\lambda r) = \frac{e^{-ik_j R}}{R} \quad , \tag{A-46}$$

where $R^2 = r^2 + (z-z')^2$, along with

$$\frac{\partial}{\partial x}\frac{e^{-ik_j R}}{R} = -\frac{e^{-ik_j R}}{R}\left[\frac{1}{R^2} + \frac{ik_j}{R}\right](x-x') \quad , \tag{A-47a}$$

$$\frac{\partial^2}{\partial x^2}\frac{e^{-ik_j R}}{R} = \frac{e^{-ik_j R}}{R}\left\{\left[\frac{3}{R} + \frac{3ik_j}{R} - k_j^2\right](x-x')^2 - \left[\frac{1}{R^2} + \frac{ik_j}{R}\right]\right\} \tag{A-47b}$$

and

$$\frac{\partial^2}{\partial x \partial y}\frac{e^{-ik_j R}}{R} = \frac{e^{-ik_j R}}{R}\left\{\left[\frac{3}{R^2} + \frac{3ik_j}{R} - k_j^2\right](x-x')(y-y')\right\} \quad . \tag{A-47c}$$

We also require (Gradshteyn and Ryzhik, 1980, p. 968)

$$\frac{\partial}{\partial x}\left[J_0(\lambda r)\right] = \frac{-(x-x')}{r} \lambda J_1(\lambda r) \tag{A-48a}$$

and

$$\frac{\partial}{\partial x}\left[J_1(\lambda r)\right] = \frac{(x-x')}{r} \lambda\left[J_0(\lambda r) - \frac{1}{\lambda r} J_1(\lambda r)\right] \quad , \tag{A-48b}$$

where $J_1(\lambda r)$ is the first order Bessel function of the first kind. From (A-48), there results

$$\frac{\partial^2}{\partial x^2}\left[J_0(\lambda r)\right] = \left[\frac{2(x-x')^2}{r^3} - \frac{1}{r}\right]\lambda J_1(\lambda r) - \left[\frac{(x-x')^2}{r^2}\right]\lambda^2 J_0(\lambda r) \tag{A-49a}$$

$$= -\left(\frac{\partial^2}{\partial y^2} + \lambda^2\right) J_0(\lambda r) \tag{A-49b}$$

and

$$\frac{\partial^2}{\partial x \partial y}\left[J_o(\lambda r)\right] = \left[\frac{2(x-x')(y-y')}{r^3}\right]\lambda J_1(\lambda r) - \left[\frac{(x-x')(y-y')}{r^2}\right]\lambda^2 J_o(\lambda r) \quad . \quad \text{(A-49c)}$$

In layer j, the particular and complementary potential solutions give rise to primary and secondary dyadic elements, i.e.,

$$\tilde{\tilde{G}}_j^E = {}^P\tilde{\tilde{G}}_j^E + {}^S\tilde{\tilde{G}}_j^E \quad \text{(A-50)}$$

and

$$\tilde{\tilde{G}}_j^H = {}^P\tilde{\tilde{G}}_j^E + {}^S\tilde{\tilde{G}}_j^E \quad . \quad \text{(A-51)}$$

Using (A-33), (A-34) and (A-43) through (A-47), the primary electric elements are

$${}^PG^E_{xxj} = \frac{1}{4\pi\hat{\gamma}_j}\left\{\left[\frac{(x-x')^2}{R^2}\right]{}^P\gamma^E_{1j} - {}^P\gamma^E_{2j} + k_j^2\,{}^P\gamma^E_{3j}\right\} \quad , \quad \text{(A-52a)}$$

$${}^PG^E_{yxj} = \frac{1}{4\pi\hat{\gamma}_j}\left\{\left[\frac{(x-x')(y-y')}{R^2}\right]{}^P\gamma^E_{1j}\right\} \quad , \quad \text{(A-52b)}$$

$${}^PG^E_{zxj} = \frac{1}{4\pi\hat{\gamma}_j}\left\{\left[\frac{(x-x')(z-z')}{R^2}\right]{}^P\gamma^E_{1j}\right\} \quad , \quad \text{(A-52c)}$$

$${}^PG^E_{xyj} = \frac{1}{4\pi\hat{\gamma}_j}\left\{\left[\frac{(x-x')(y-y')}{R^2}\right]{}^P\gamma^E_{1j}\right\} \quad , \quad \text{(A-52d)}$$

$${}^PG^E_{yyj} = \frac{1}{4\pi\hat{\gamma}_j}\left\{\left[\frac{(y-y')^2}{R^2}\right]{}^P\gamma^E_{1j} - {}^P\gamma^E_{2j} + k_j^2\,{}^P\gamma^E_{3j}\right\} \quad , \quad \text{(A-52e)}$$

$${}^PG^E_{zyj} = \frac{1}{4\pi\hat{\gamma}_j}\left\{\left[\frac{(y-y')(z-z')}{R^2}\right]{}^P\gamma^E_{1j}\right\} \quad , \quad \text{(A-52f)}$$

$${}^PG^E_{xzj} = \frac{1}{4\pi\hat{\gamma}_j}\left\{\left[\frac{(x-x')(z-z')}{R^2}\right]{}^P\gamma^E_{1j}\right\} \quad , \quad \text{(A-52g)}$$

$${}^PG^E_{yzj} = \frac{1}{4\pi\hat{\gamma}_j}\left\{\left[\frac{(y-y')(z-z')}{R^2}\right]{}^P\gamma^E_{1j}\right\} \quad \text{(A-52h)}$$

and

$$ {}^{P}G^{E}_{zzj} = \frac{1}{4\pi\hat{\gamma}_j}\left\{\left[\frac{(z-z')^2}{R^2}\right]{}^{P}\gamma^{E}_{1j} - {}^{P}\gamma^{E}_{2j} + k_j^2\,{}^{P}\gamma^{E}_{3j}\right\} \quad , \quad \text{(A-52i)} $$

where

$$ {}^{P}\gamma^{E}_{1j} = \frac{e^{-ik_jR}}{R}\left[\frac{3}{R^2} + \frac{3ik_j}{R} - k_j^2\right] \quad , \quad \text{(A-53a)} $$

$$ {}^{P}\gamma^{E}_{2j} = \frac{e^{-ik_jR}}{R}\left[\frac{1}{R^2} + \frac{ik_j}{R}\right] \quad \text{(A-53b)} $$

and

$$ {}^{P}\gamma^{E}_{3j} = \frac{e^{-ik_jR}}{R} \quad . \quad \text{(A-53c)} $$

We have returned to consideration of J_y to specify all nine tensor members. From (A-33), (A-34), (A-43), (A-48) and (A-49), the secondary electric elements are

$$ {}^{s}G^{E}_{xxj} = \frac{1}{4\pi\hat{\gamma}_j}\left\{\left[\frac{2(x-x')^2}{r^3} - \frac{1}{r}\right]{}^{s}\gamma^{E}_{1j} - \left[\frac{(x-x')^2}{r^2}\right]{}^{s}\gamma^{E}_{2j} + k_j^2\,{}^{s}\gamma^{E}_{3j}\right\} \quad , \quad \text{(A-54a)} $$

$$ {}^{s}G^{E}_{yxj} = \frac{1}{4\pi\hat{\gamma}_j}\left\{\left[\frac{2(x-x')(y-y')}{r^3}\right]{}^{s}\gamma^{E}_{1j} - \left[\frac{(x-x')(y-y')}{r^2}\right]{}^{s}\gamma^{E}_{2j}\right\} \quad , \quad \text{(A-54b)} $$

$$ {}^{s}G^{E}_{zxj} = \frac{1}{4\pi\hat{\gamma}_j}\left\{\left[\frac{-(x-x')}{r}\right]{}^{s}\gamma^{E}_{4j}\right\} \quad , \quad \text{(A-54c)} $$

$$ {}^{s}G^{E}_{xyj} = \frac{1}{4\pi\hat{\gamma}_j}\left\{\left[\frac{2(x-x')(y-y')}{r^3}\right]{}^{s}\gamma^{E}_{1j} - \left[\frac{(x-x')(y-y')}{r^2}\right]{}^{s}\gamma^{E}_{2j}\right\} \quad , \quad \text{(A-54d)} $$

$$ {}^{s}G^{E}_{yyj} = \frac{1}{4\pi\hat{\gamma}_j}\left\{\left[\frac{2(y-y')^2}{r^3} - \frac{1}{r}\right]{}^{s}\gamma^{E}_{1j} - \left[\frac{(y-y')^2}{r^2}\right]{}^{s}\gamma^{E}_{2j} + k_j^2\,{}^{s}\gamma^{E}_{3j}\right\} \quad , \quad \text{(A-54e)} $$

$$ {}^{s}G^{E}_{zyj} = \frac{1}{4\pi\hat{\gamma}_j}\left\{\left[\frac{-(y-y')}{r}\right]{}^{s}\gamma^{E}_{4j}\right\} \quad , \quad \text{(A-54f)} $$

$$ {}^{s}G^{E}_{xzj} = \frac{1}{4\pi\hat{\gamma}_j}\left\{\left[\frac{-(x-x')}{r}\right]{}^{s}\gamma^{E}_{4j}\right\} \quad , \quad \text{(A-54g)} $$

$$ {}^{s}G^{E}_{yzj} = \frac{1}{4\pi\hat{\gamma}_j}\left\{\left[\frac{-(y-y')}{r}\right]{}^{s}\gamma^{E}_{6j}\right\} \qquad \text{(A-54h)} $$

and

$$ {}^{s}G^{E}_{zzj} = \frac{1}{4\pi\hat{\gamma}_j}\left\{\gamma^{E}_{5j}\right\} \quad , \qquad \text{(A-54i)} $$

with Hankel transforms

$$ {}^{s}\gamma^{E}_{1j} = \int_0^\infty \Big\{\Big[u_j {}^{x}A^{TM}_{j} + \frac{k_j^2}{u_j}{}^{x}A^{TE}_{j}\Big]e^{+u_j(z-d_{j-1})} - \Big[u_j\big(e^{-u_j(z'-d_{j-1})} + {}^{x}A^{TM}_{j}\big)^{-}R^{TM}_{j} - \frac{k_j^2}{u_j}\big(e^{-u_j(z'-d_{j-1})} + {}^{x}A^{TE}_{j}\big)^{-}R^{TE}_{j}\Big]e^{-u_j(z-d_{j-1})}\Big\} J_1(\lambda r)\,d\lambda \quad , \qquad \text{(A-55a)} $$

$$ {}^{s}\gamma^{E}_{2j} = \int_0^\infty \Big\{\Big[u_j {}^{x}A^{TM}_{j} + \frac{k_j^2}{u_j}{}^{x}A^{TE}_{j}\Big]e^{+u_j(z-d_{j-1})} - \Big[u_j\big(e^{-u_j(z'-d_{j-1})} + {}^{x}A^{TM}_{j}\big)^{-}R^{TM}_{j} - \frac{k_j^2}{u_j}\big(e^{-u_j(z'-d_{j-1})} + {}^{x}A^{TE}_{j}\big)^{-}R^{TE}_{j}\Big]e^{-u_j(z-d_{j-1})}\Big\} \lambda J_0(\lambda r)\,d\lambda \quad , \qquad \text{(A-55b)} $$

$$ {}^{s}\gamma^{E}_{3j} = \int_0^\infty \frac{1}{u_j}\Big\{\Big[{}^{x}A^{TE}_{j}\Big]e^{+u_j(z-d_{j-1})} + \Big[\big(e^{-u_j(z'-d_{j-1})} + {}^{x}A^{TE}_{j}\big)^{-}R^{TE}_{j}\Big]e^{-u_j(z-d_{j-1})}\Big\} \lambda J_0(\lambda r)\,d\lambda \quad , \qquad \text{(A-55c)} $$

$$ {}^{s}\gamma^{E}_{4j} = \int_0^\infty \lambda^2\Big\{\Big[{}^{x}A^{TM}_{j}\Big]e^{+u_j(z-d_{j-1})} + \Big[\big(e^{-u_j(z'-d_{j-1})} + {}^{x}A^{TM}_{j}\big)^{-}R^{TM}_{j}\Big]e^{-u_j(z-d_{j-1})}\Big\} J_1(\lambda r)\,d\lambda \quad , \qquad \text{(A-55d)} $$

$$ {}^{s}\gamma^{E}_{5j} = \int_0^\infty \frac{\lambda^2}{u_j}\Big\{\Big[{}^{z}A^{TM}_{j}\Big]e^{+u_j(z-d_{j-1})} + \Big[\big(e^{-u_j(z'-d_{j-1})} + {}^{z}A^{TM}_{j}\big)^{-}R^{TM}_{j}\Big]e^{-u_j(z-d_{j-1})}\Big\} \lambda J_0(\lambda r)\,d\lambda \qquad \text{(A-55e)} $$

and

$$ {}^{s}\gamma^{E}_{6j} = \int_0^\infty \lambda^2\Big\{\Big[{}^{z}A^{TM}_{j}\Big]e^{+u_j(z-d_{j-1})} - \Big[\big(e^{-u_j(z'-d_{j-1})} + {}^{z}A^{TM}_{j}\big)^{-}R^{TM}_{j}\Big]e^{-u_j(z-d_{j-1})}\Big\} J_1(\lambda r)\,d\lambda \quad . \qquad \text{(A-55f)} $$

Similarly, the primary magnetic members become

$$ {}^{P}G^{H}_{xxj} = 0 \quad , \qquad \text{(A-56a)} $$

$$ {}^{P}G^{H}_{yxj} = \frac{-1}{4\pi}(z-z')\,{}^{P}\gamma^{H}_{1j} \quad , \qquad \text{(A-56b)} $$

$$ {}^{P}G^{H}_{zxj} = \frac{1}{4\pi}(y-y')\,{}^{P}\gamma^{H}_{1j} \quad , \qquad \text{(A-56c)} $$

$$ {}^{P}G^{H}_{xyj} = \frac{1}{4\pi}(z-z')\,{}^{P}\gamma^{H}_{1j} \quad , \quad \text{(A-56d)} $$

$$ {}^{P}G^{H}_{yyj} = 0 \quad , \quad \text{(A-56e)} $$

$$ {}^{P}G^{H}_{zyj} = \frac{-1}{4\pi}(x-x')\,{}^{P}\gamma^{H}_{1j} \quad , \quad \text{(A-56f)} $$

$$ {}^{P}G^{H}_{xzj} = \frac{-1}{4\pi}(y-y')\,{}^{P}\gamma^{H}_{1j} \quad , \quad \text{(A-56g)} $$

$$ {}^{P}G^{H}_{yzj} = \frac{1}{4\pi}(x-x')\,{}^{P}\gamma^{H}_{1j} \quad \text{(A-56h)} $$

and

$$ {}^{P}G^{H}_{zzj} = 0 \quad , \quad \text{(A-56i)} $$

where

$$ {}^{P}\gamma^{H}_{1j} = \frac{e^{-ik_jR}}{R}\left[\frac{1}{R^2} + \frac{ik_j}{R}\right] \quad . \quad \text{(A-57)} $$

The secondary elements here are

$$ {}^{S}G^{H}_{xxj} = \frac{1}{4\pi}\left\{\left[\frac{2(x-x')(y-y')}{r^3}\right]{}^{S}\gamma^{H}_{1j} - \left[\frac{(x-x')(y-y')}{r^2}\right]{}^{S}\gamma^{H}_{2j}\right\} \quad , \quad \text{(A-58a)} $$

$$ {}^{S}G^{H}_{yxj} = \frac{1}{4\pi}\left\{-\left[\frac{2(x-x')^2}{r^3} - \frac{1}{r}\right]{}^{S}\gamma^{H}_{1j} + \left[\frac{(x-x')^2}{r^2}\right]{}^{S}\gamma^{H}_{2j} + {}^{S}\gamma^{H}_{3j}\right\} \quad , \quad \text{(A-58b)} $$

$$ {}^{S}G^{H}_{zxj} = \frac{1}{4\pi}\left\{\left[\frac{(y-y')}{r}\right]{}^{S}\gamma^{H}_{4j}\right\} \quad , \quad \text{(A-58c)} $$

$$ {}^{S}G^{H}_{xyj} = \frac{-1}{4\pi}\left\{-\left[\frac{2(y-y')^2}{r^3} - \frac{1}{r}\right]{}^{S}\gamma^{H}_{1j} + \left[\frac{(y-y')^2}{r^2}\right]{}^{S}\gamma^{H}_{2j} + {}^{S}\gamma^{H}_{3j}\right\} \quad , \quad \text{(A-58d)} $$

$$ {}^{S}G^{H}_{yyj} = \frac{-1}{4\pi}\left\{\left[\frac{2(x-x')(y-y')}{r^3}\right]{}^{S}\gamma^{H}_{1j} - \left[\frac{(x-x')(y-y')}{r^2}\right]{}^{S}\gamma^{H}_{2j}\right\} \quad , \quad \text{(A-58e)} $$

$$G^H_{zy_i} = \frac{1}{4\pi}\left\{-\left[\frac{(x-x')}{r}\right]{}^s\gamma^H_{4j}\right\} \quad , \quad \text{(A-58f)}$$

$${}^sG^H_{xz_j} = \frac{1}{4\pi}\left\{-\left[\frac{(y-y')}{r}\right]{}^s\gamma^H_{5j}\right\} \quad , \quad \text{(A-58g)}$$

$${}^sG^H_{yz_j} = \frac{1}{4\pi}\left\{\left[\frac{(x-x')}{r}\right]{}^s\gamma^H_{5j}\right\} \quad \text{(A-58h)}$$

and

$${}^sG^H_{zz_j} = 0 \quad , \quad \text{(A-58i)}$$

with transforms

$${}^s\gamma^H_{1j} = \int_0^\infty \{[{}^xA^{TM}_j - {}^xA^{TE}_j]e^{+u_j(z-d_{j-1})} + [(e^{-u_j(z'-d_{j-1})} + {}^xA^{TM}_j)^- R^{TM}_j + (e^{-u_j(z'-d_{j-1})} + {}^xA^{TE}_j)^- R^{TE}_j]e^{-u_j(z-d_{j-1})}\} J_1(\lambda r)\, d\lambda \quad , \quad \text{(A-59a)}$$

$${}^s\gamma^H_{2j} = \int_0^\infty \{[{}^xA^{TM}_j - {}^xA^{TE}_j]e^{+u_j(z-d_{j-1})} + [(e^{-u_j(z'-d_{j-1})} + {}^xA^{TM}_j)^- R^{TM}_j + (e^{-u_j(z'-d_{j-1})} + {}^xA^{TE}_j)^- R^{TE}_j]e^{-u_j(z-d_{j-1})}\} \lambda J_0(\lambda r)\, d\lambda \quad , \quad \text{(A-59b)}$$

$${}^s\gamma^H_{3j} = \int_0^\infty \{[{}^xA^{TE}_j]e^{+u_j(z-d_{j-1})} - [(e^{-u_j(z'-d_{j-1})} + {}^xA^{TE}_j)^- R^{TE}_j]e^{-u_j(z-d_{j-1})}\} \lambda J_0(\lambda r)\, d\lambda \quad , \quad \text{(A-59c)}$$

$${}^s\gamma^H_{4j} = \int_0^\infty \frac{\lambda^2}{u_j}\{[{}^xA^{TE}_j]e^{+u_j(z-d_{j-1})} + [(e^{-u_j(z'-d_{j-1})} + {}^xA^{TE}_j)^- R^{TE}_j]e^{-u_j(z-d_{j-1})}\} J_1(\lambda r)\, d\lambda \quad \text{(A-59d)}$$

and

$${}^s\gamma^H_{5j} = \int_0^\infty \frac{\lambda^2}{u_j}\{[{}^zA^{TM}_j]e^{+u_j(z-d_{j-1})} + [(e^{-u_j(z'-d_{j-1})} + {}^xA^{TM}_j)^- R^{TM}_j]e^{-u_j(z-d_{j-1})}\} J_1(\lambda r)\, d\lambda \quad . \quad \text{(A-59e)}$$

Since just complementary potential solutions exist in layers other than that containing the source, only secondary Green's function elements are defined. The forms of the secondary elements are identical to equations (A-54) and (A-58), with l substituted for j everywhere, and

will not be rewritten. The pertinent Hankel transforms for the electric elements, for $i > j$, are

$$ {}^{s}\gamma^{E}_{ij} = \int_0^\infty \{ [u_i {}^{+}B^{TM}_{ij} ({}^{x}A^{TM}_{j} e^{+u_j h_j} / {}^{+}R^{TM}_{j}) {}^{+}R^{TM}_{i} + \frac{k_z^2}{u_j} {}^{+}B^{TE}_{ij} ({}^{x}A^{TE}_{j} e^{+u_j h_j} / {}^{+}R^{TE}_{j}) {}^{+}R^{TE}_{i}] e^{+u_i (z-d_i)} $$
$$ - [u_i {}^{+}B^{TM}_{ij} ({}^{x}A^{TM}_{j} e^{+u_j h_j} / {}^{+}R^{TM}_{j}) - \frac{k_z^2}{u_j} {}^{+}B^{TE}_{ij} ({}^{x}A^{TE}_{j} e^{+u_j h_j} / {}^{+}R^{TE}_{j})] e^{-u_i (z-d_i)} \} J_1(\lambda r) d\lambda \quad , \quad \text{(A-60a)} $$

$$ {}^{s}\gamma^{E}_{zj} = \int_0^\infty \{ [u_i {}^{+}B^{TM}_{ij} ({}^{x}A^{TM}_{j} e^{+u_j h_j} / {}^{+}R^{TM}_{j}) {}^{+}R^{TM}_{i} + \frac{k_z^2}{u_j} {}^{+}B^{TE}_{ij} ({}^{x}A^{TE}_{j} e^{+u_j h_j} / {}^{+}R^{TE}_{j}) {}^{+}R^{TE}_{i}] e^{+u_i (z-d_i)} $$
$$ - [u_i {}^{+}B^{TM}_{ij} ({}^{x}A^{TM}_{j} e^{+u_j h_j} / {}^{+}R^{TM}_{j}) - \frac{k_z^2}{u_j} {}^{+}B^{TE}_{ij} ({}^{x}A^{TE}_{j} e^{+u_j h_j} / {}^{+}R^{TE}_{j})] e^{-u_i (z-d_i)} \} \lambda J_0(\lambda r) d\lambda \quad , \quad \text{(A-60b)} $$

$$ {}^{s}\gamma^{E}_{3j} = \int_0^\infty \frac{1}{u_j} \{ [{}^{+}B^{TE}_{ij} ({}^{x}A^{TE}_{j} e^{+u_j h_j} / {}^{+}R^{TE}_{j})] [{}^{+}R^{TE}_{i} e^{+u_i (z-d_i)} + e^{-u_i (z-d_i)}] \} \lambda J_0(\lambda r) d\lambda \quad , \quad \text{(A-60c)} $$

$$ {}^{s}\gamma^{E}_{4j} = \int_0^\infty \lambda^2 \{ [{}^{+}B^{TM}_{ij} ({}^{x}A^{TM}_{j} e^{+u_j h_j} / {}^{+}R^{TM}_{j})] [{}^{+}R^{TM}_{i} e^{+u_i (z-d_i)} + e^{-u_i (z-d_i)}] \} J_1(\lambda r) d\lambda \quad , \quad \text{(A-60d)} $$

$$ {}^{s}\gamma^{E}_{5j} = \int_0^\infty \frac{\lambda^2}{u_j} \{ [{}^{+}B^{TM}_{ij} ({}^{z}A^{TM}_{j} e^{+u_j h_j} / {}^{+}R^{TM}_{j})] [{}^{+}R^{TM}_{i} e^{+u_i (z-d_i)} + e^{-u_i (z-d_i)}] \} \lambda J_0(\lambda r) d\lambda \quad \text{(A-60e)} $$

and

$$ {}^{s}\gamma^{E}_{6j} = \int_0^\infty \lambda^2 \frac{u_i}{u_j} \{ [{}^{+}B^{TM}_{ij} ({}^{z}A^{TM}_{j} e^{+u_j h_j} / {}^{+}R^{TM}_{j})] [{}^{+}R^{TM}_{i} e^{+u_i (z-d_i)} - e^{-u_i (z-d_i)}] \} J_1(\lambda r) d\lambda \quad . \quad \text{(A-60f)} $$

The magnetic transforms are

$$ {}^{s}\gamma^{H}_{ij} = \int_0^\infty \{ [{}^{+}B^{TM}_{ij} ({}^{x}A^{TM}_{j} e^{+u_j h_j} / {}^{+}R^{TM}_{j}) {}^{+}R^{TM}_{i} - \frac{\hat{z}_j u_i}{\hat{z}_i u_j} {}^{+}B^{TE}_{ij} ({}^{x}A^{TE}_{j} e^{+u_j h_j} / {}^{+}R^{TE}_{j}) {}^{+}R^{TE}_{i}] e^{+u_i (z-d_i)} $$
$$ + [{}^{+}B^{TM}_{ij} ({}^{x}A^{TM}_{j} e^{+u_j h_j} / {}^{+}R^{TM}_{j}) + \frac{\hat{z}_j u_i}{\hat{z}_i u_j} {}^{+}B^{TE}_{ij} ({}^{x}A^{TE}_{j} e^{+u_j h_j} / {}^{+}R^{TE}_{j})] e^{-u_i (z-d_i)} \} J_1(\lambda r) d\lambda \quad , \quad \text{(A-61a)} $$

$$ {}^{s}\gamma^{H}_{2j} = \int_0^\infty \{ [{}^{+}B^{TM}_{ij} ({}^{x}A^{TM}_{j} e^{+u_j h_j} / {}^{+}R^{TM}_{j}) {}^{+}R^{TM}_{i} - \frac{\hat{z}_j u_i}{\hat{z}_i u_j} {}^{+}B^{TE}_{ij} ({}^{x}A^{TE}_{j} e^{+u_j h_j} / {}^{+}R^{TE}_{j}) {}^{+}R^{TE}] e^{+u_i (z-d_i)} $$
$$ + [{}^{+}B^{TM}_{ij} ({}^{x}A^{TM}_{j} e^{+u_j h_j} / {}^{+}R^{TM}_{j}) + \frac{\hat{z}_j u_i}{\hat{z}_i u_j} {}^{+}B^{TE}_{ij} ({}^{x}A^{TE}_{j} e^{+u_j h_j} / {}^{+}R^{TE}_{j})] e^{-u_i (z-d_i)} \} \lambda J_0(\lambda r) d\lambda \quad , \quad \text{(A-61b)} $$

$$ {}^{s}\gamma^{H}_{3j} = \int_0^\infty \frac{\hat{z}_j u_i}{\hat{z}_i u_j} \{ [{}^{+}B^{TE}_{ij} ({}^{x}A^{TE}_{j} e^{+u_j h_j} / {}^{+}R^{TE}_{j})] [{}^{+}R^{TE}_{i} e^{+u_i (z-d_i)} - e^{-u_i (z-d_i)}] \} \lambda J_0(\lambda r) d\lambda \quad , \quad \text{(A-61c)} $$

$$ {}^{s}\gamma^{H}_{4z} = \int_0^\infty \frac{\hat{z}_j \lambda^2}{\hat{z}_z u_j} \{[{}^{+}B^{TE}_{zj}({}^{x}A^{TE}_{j} e^{+u_j h_j}/{}^{+}R^{TE}_{j})][{}^{+}R^{TE}_{z} e^{+u_z(z-d_z)} + e^{-u_z(z-d_z)}]\} J_1(\lambda r) d\lambda \qquad \text{(A-61d)} $$

and

$$ {}^{s}\gamma^{H}_{5z} = \int_0^\infty \frac{\lambda^2}{u_j} \{[{}^{+}B^{TM}_{zj}({}^{z}A^{TM}_{j} e^{+u_j h_j}/{}^{+}R^{TM}_{j})][{}^{+}R^{TM}_{z} e^{+u_z(z-d_z)} + e^{-u_z(z-d_z)}]\} J_1(\lambda r) d\lambda \qquad \text{(A-61e)} $$

For receivers in the basal half-space, the transforms simplify to

$$ {}^{s}\gamma^{E}_{1n} = \int_0^\infty -\{[u_n {}^{+}B^{TM}_{nj}({}^{x}A^{TM}_{j} e^{+u_j h_j}/{}^{+}R^{TM}_{j}) + \frac{k_n^2}{u_j} {}^{+}B^{TE}_{nj}({}^{x}A^{TE}_{j} e^{+u_j h_j}/{}^{+}R^{TE}_{j})] e^{-u_n(z-d_{n-1})}\} J_1(\lambda r) d\lambda \qquad \text{(A-62a)} $$

$$ {}^{s}\gamma^{E}_{2n} = \int_0^\infty -\{[u_n {}^{+}B^{TM}_{nj}({}^{x}A^{TM}_{j} e^{+u_j h_j}/{}^{+}R^{TM}_{j}) + \frac{k_n^2}{u_j} {}^{+}B^{TE}_{nj}({}^{x}A^{TE}_{j} e^{+u_j h_j}/{}^{+}R^{TE}_{j})] e^{-u_n(z-d_{n-1})}\} \lambda J_0(\lambda r) d\lambda \qquad \text{(A-62b)} $$

$$ {}^{s}\gamma^{E}_{3n} = \int_0^\infty \frac{1}{u_j} \{[{}^{+}B^{TE}_{nj}({}^{x}A^{TE}_{j} e^{+u_j h_j}/{}^{+}R^{TE}_{j})] e^{-u_n(z-d_{n-1})}\} \lambda J_0(\lambda r) d\lambda \qquad \text{(A-62c)} $$

$$ {}^{s}\gamma^{E}_{4n} = \int_0^\infty \lambda^2 \{[{}^{+}B^{TM}_{nj}({}^{x}A^{TM}_{j} e^{+u_j h_j}/{}^{+}R^{TM}_{j})] e^{-u_n(z-d_{n-1})}\} J_1(\lambda r) d\lambda \qquad \text{(A-62d)} $$

$$ {}^{s}\gamma^{E}_{5n} = \int_0^\infty \frac{\lambda^2}{u_j} \{[{}^{+}B^{TM}_{nj}({}^{z}A^{TM}_{j} e^{+u_j h_j}/{}^{+}R^{TM}_{j})] e^{-u_n(z-d_{n-1})}\} \lambda J_0(\lambda r) d\lambda \qquad \text{(A-62e)} $$

and

$$ {}^{s}\gamma^{E}_{6n} = \int_0^\infty \lambda^2 \frac{u_n}{u_j} \{[{}^{+}B^{TM}_{nj}({}^{z}A^{TM}_{j} e^{+u_j h_j}/{}^{+}R^{TM}_{j})] e^{-u_n(z-d_{n-1})}\} J_1(\lambda r) d\lambda \qquad \text{(A-62f)} $$

along with

$$ {}^{s}\gamma^{H}_{1n} = \int_0^\infty \{[{}^{+}B^{TM}_{nj}({}^{x}A^{TM}_{j} e^{+u_j h_j}/{}^{+}R^{TM}_{j}) + \frac{\hat{z}_j u_n}{\hat{z}_n u_j} {}^{+}B^{TE}_{nj}({}^{x}A^{TE}_{j} e^{+u_j h_j}/{}^{+}R^{TE}_{j})] e^{-u_n(z-d_{n-1})}\} J_1(\lambda r) d\lambda \qquad \text{(A-63a)} $$

$$ {}^{s}\gamma^{H}_{2n} = \int_0^\infty \{[{}^{+}B^{TM}_{nj}({}^{x}A^{TM}_{j} e^{+u_j h_j}/{}^{+}R^{TM}_{j}) + \frac{\hat{z}_j u_n}{\hat{z}_n u_j} {}^{+}B^{TE}_{nj}({}^{x}A^{TE}_{j} e^{+u_j h_j}/{}^{+}R^{TE}_{j})] e^{-u_n(z-d_{n-1})}\} \lambda J_0(\lambda r) d\lambda \quad , \quad \text{(A-63b)} $$

$$ {}^{s}\gamma^{H}_{3n} = \int_0^\infty \frac{\hat{z}_j u_n}{\hat{z}_n u_j} \{[{}^{+}B^{TE}_{nj}({}^{x}A^{TE}_{j} e^{+u_j h_j}/{}^{+}R^{TE}_{j})] e^{-u_n(z-d_{n-1})}\} \lambda J_0(\lambda r) d\lambda \quad , \quad \text{(A-63c)} $$

$$ {}^{s}\gamma^{H}_{4n} = \int_0^\infty \frac{\hat{z}_j u_n}{\hat{z}_n u_j} \{[{}^{+}B^{TE}_{nj}({}^{x}A^{TE}_{j} e^{+u_j h_j}/{}^{+}R^{TE}_{j})] e^{-u_n(z-d_{n-1})}\} J_1(\lambda r) d\lambda \quad \text{(A-63d)} $$

and

$$ {}^{s}\gamma^{H}_{5n} = \int_0^\infty \frac{\lambda^2}{u_j} \{[{}^{+}B^{TM}_{nj}({}^{z}A^{TM}_{j} e^{+u_j h_j}/{}^{+}R^{TM}_{j})] e^{-u_n(z-d_{n-1})}\} J_1(\lambda r) d\lambda \quad , \quad \text{(A-63e)} $$

where ${}^{+}B^{TM}_{nj} = [1 + {}^{+}R^{TM}_{n-1}]\,{}^{+}B^{TM}_{n-1j}$ and ${}^{+}B^{TE}_{nj} = [1 + {}^{+}R^{TE}_{n-1}]\,{}^{+}B^{TE}_{n-1j}$.

In layer $l < j$, the electric Hankel transforms are

$$ {}^{s}\gamma^{E}_{1l} = \int_0^\infty \{[u_l {}^{-}B^{TM}_{lj}(e^{-u_j(z'-d_{j-1})} + {}^{x}A^{TM}_{j}) + \frac{k_l^2}{u_j} {}^{-}B^{TE}_{lj}(e^{-u_j(z'-d_{j-1})} + {}^{x}A^{TE}_{j})] e^{+u_l(z-d_{l-1})} $$
$$ - [u_l {}^{-}B^{TM}_{lj}(e^{-u_j(z'-d_{j-1})} + {}^{x}A^{TM}_{j}) {}^{-}R^{TM}_{l} - \frac{k_l^2}{u_j} {}^{-}B^{TE}_{lj}(e^{-u_j(z'-d_{j-1})} + {}^{x}A^{TE}_{j}) {}^{-}R^{TE}_{l}] e^{-u_l(z-d_{l-1})}] J_1(\lambda r) d\lambda \quad , \quad \text{(A-64a)} $$

$$ {}^{s}\gamma^{E}_{2l} = \int_0^\infty \{[u_l {}^{-}B^{TM}_{lj}(e^{-u_j(z'-d_{j-1})} + {}^{x}A^{TM}_{j}) + \frac{k_l^2}{u_j} {}^{-}B^{TE}_{lj}(e^{-u_j(z'-d_{j-1})} + {}^{x}A^{TE}_{j})] e^{+u_l(z-d_{l-1})} $$
$$ - [u_l {}^{-}B^{TM}_{lj}(e^{-u_j(z'-d_{j-1})} + {}^{x}A^{TM}_{j}) {}^{-}R^{TM}_{l} - \frac{k_l^2}{u_j} {}^{-}B^{TE}_{lj}(e^{-u_j(z'-d_{j-1})} + {}^{x}A^{TE}_{j}) {}^{-}R^{TE}_{l}] e^{-u_l(z-d_{l-1})}] \lambda J_0(\lambda r) d\lambda \quad , \quad \text{(A-64b)} $$

$$ {}^{s}\gamma^{E}_{3l} = \int_0^\infty \frac{1}{u_j} \{[{}^{-}B^{TE}_{lj}(e^{-u_j(z'-d_{j-1})} + {}^{x}A^{TE}_{j})][e^{+u_l(z-d_{l-1})} + {}^{-}R^{TE}_{l} e^{-u_l(z-d_{l-1})}]\} \lambda J_0(\lambda r) d\lambda \quad , \quad \text{(A-64c)} $$

$$ {}^{s}\gamma^{E}_{4l} = \int_0^\infty \lambda^2 \{[{}^{-}B^{TM}_{lj}(e^{-u_j(z'-d_{j-1})} + {}^{x}A^{TM}_{j})][e^{+u_l(z-d_{l-1})} + {}^{-}R^{TM}_{l} e^{-u_l(z-d_{l-1})}]\} J_1(\lambda r) d\lambda \quad , \quad \text{(A-64d)} $$

$$ {}^{s}\gamma^{H}_{5l} = \int_0^\infty \frac{\lambda^2}{u_j} \{[{}^{-}B^{TM}_{lj}(e^{-u_j(z'-d_{j-1})} + {}^{z}A^{TM}_{j})][e^{+u_l(z-d_{l-1})} + {}^{-}R^{TM}_{l} e^{-u_l(z-d_{l-1})}]\} \lambda J_0(\lambda r) d\lambda \quad \text{(A-64e)} $$

and

$$ {}^{s}\gamma^{H}_{6l} = \int_0^\infty \lambda^2 \frac{u_l}{u_j} \{[{}^{-}B^{TM}_{lj}(e^{-u_j(z'-d_{j-1})} + {}^{z}A^{TM}_{j})][e^{+u_l(z-d_{l-1})} - {}^{-}R^{TM}_{l} e^{-u_l(z-d_{l-1})}]\} J_1(\lambda r) d\lambda \quad , \quad \text{(A-64f)} $$

with the magnetic integrals

$$ {}^{s}Y^{H}_{12} = \int_0^\infty \{ [{}^{-}B^{TM}_{zj} (e^{-u_j(z'-d_{j-1})} + {}^{x}A^{TM}_{j}) - \frac{\hat{z}_j u_z}{\hat{z}_z u_j} {}^{-}B^{TE}_{zj} (e^{-u_j(z'-d_{j-1})} + {}^{x}A^{TE}_{j})] e^{+u_z(z-d_{z-1})} $$
$$ + [{}^{-}B^{TM}_{zj} (e^{-u_j(z'-d_{j-1})} + {}^{x}A^{TM}_{j}) {}^{-}R^{TM}_{z} + \frac{\hat{z}_j u_z}{\hat{z}_z u_j} {}^{-}B^{TE}_{zj} (e^{-u_j(z'-d_{j-1})} + {}^{x}A^{TE}_{j}) {}^{-}R^{TE}_{z}] e^{-u_z(z-d_{z-1})} \} J_1(\lambda r) d\lambda \quad , \quad \text{(A-65a)} $$

$$ {}^{s}Y^{H}_{22} = \int_0^\infty \{ [{}^{-}B^{TM}_{zj} (e^{-u_j(z'-d_{j-1})} + {}^{x}A^{TM}_{j}) - \frac{\hat{z}_j u_z}{\hat{z}_z u_j} {}^{-}B^{TE}_{zj} (e^{-u_j(z'-d_{j-1})} + {}^{x}A^{TE}_{j})] e^{+u_z(z-d_{z-1})} $$
$$ + [{}^{-}B^{TM}_{zj} (e^{-u_j(z'-d_{j-1})} + {}^{x}A^{TM}_{j}) {}^{-}R^{TM}_{z} + \frac{\hat{z}_j u_z}{\hat{z}_z u_j} {}^{-}B^{TE}_{zj} (e^{-u_j(z'-d_{j-1})} + {}^{x}A^{TE}_{j}) {}^{-}R^{TE}_{z}] e^{-u_z(z-d_{z-1})} \} \lambda J_0(\lambda r) d\lambda \quad , \quad \text{(A-65b)} $$

$$ {}^{s}Y^{H}_{32} = \int_0^\infty \frac{\hat{z}_j u_z}{\hat{z}_z u_j} \{ [{}^{-}B^{TE}_{zj} (e^{-u_j(z'-d_{j-1})} + {}^{x}A^{TE}_{j})] [e^{+u_z(z-d_{z-1})} - {}^{-}R^{TE}_{z} e^{-u_z(z-d_{z-1})}] \} \lambda J_0(\lambda r) d\lambda \quad , \quad \text{(A-65c)} $$

$$ {}^{s}Y^{H}_{42} = \int_0^\infty \frac{\hat{z}_j u_z}{\hat{z}_z u_j} \{ [{}^{-}B^{TM}_{zj} (e^{-u_j(z'-d_{j-1})} + {}^{x}A^{TM}_{j})] [e^{+u_z(z-d_{z-1})} + {}^{-}R^{TM}_{z} e^{-u_z(z-d_{z-1})}] \} J_1(\lambda r) d\lambda \quad \text{(A-65d)} $$

and

$$ {}^{s}Y^{H}_{52} = \int_0^\infty \frac{\lambda^2}{u_j} \{ [{}^{-}B^{TM}_{zj} (e^{-u_j(z'-d_{j-1})} + {}^{z}A^{TM}_{j})] [e^{+u_z(z-d_{z-1})} + {}^{-}R^{TM}_{z} e^{-u_z(z-d_{z-1})}] \} J_1(\lambda r) d\lambda \quad . \quad \text{(A-65e)} $$

Finally, for fields in the air, the transforms become

$$ {}^{s}Y^{E}_{10} = \int_0^\infty \{ [u_o {}^{-}B^{TM}_{oj} (e^{-u_j(z'-d_{j-1})} + {}^{x}A^{TM}_{j}) + \frac{k_o^2}{u_j} {}^{-}B^{TE}_{oj} (e^{-u_j(z'-d_{j-1})} + {}^{x}A^{TE}_{j})] e^{+u_o z} \} J_1(\lambda r) d\lambda \quad , \quad \text{(A-66a)} $$

$$ {}^{s}Y^{E}_{20} = \int_0^\infty \{ [u_o {}^{-}B^{TM}_{oj} (e^{-u_j(z'-d_{j-1})} + {}^{x}A^{TM}_{j}) + \frac{k_o^2}{u_j} {}^{-}B^{TE}_{oj} (e^{-u_j(z'-d_{j-1})} + {}^{x}A^{TE}_{j})] e^{+u_o z} \} \lambda J_0(\lambda r) d\lambda \quad , \quad \text{(A-66b)} $$

$$ {}^{s}Y^{E}_{30} = \int_0^\infty \frac{1}{u_j} \{ [{}^{-}B^{TE}_{oj} (e^{-u_j(z'-d_{j-1})} + {}^{x}A^{TE}_{j})] e^{+u_o z} \} \lambda J_0(\lambda r) d\lambda \quad , \quad \text{(A-66c)} $$

$$ {}^{s}Y^{E}_{40} = \int_0^\infty \lambda^2 \{ [{}^{-}B^{TM}_{oj} (e^{-u_j(z'-d_{j-1})} + {}^{x}A^{TM}_{j})] e^{+u_o z} \} J_1(\lambda r) d\lambda \quad , \quad \text{(A-66d)} $$

$$ {}^{s}Y^{E}_{50} = \int_0^\infty \frac{\lambda^2}{u_j} \{ [{}^{-}B^{TM}_{oj} (e^{-u_j(z'-d_{j-1})} + {}^{z}A^{TM}_{j})] e^{+u_o z} \} \lambda J_0(\lambda r) d\lambda \quad \text{(A-66e)} $$

and

$$ {}^{s}Y^{E}_{6o} = \int_0^\infty \lambda^2 \frac{u_o}{u_j} \{[{}^{-}B^{TM}_{oj}(e^{-u_j(z'-d_{j-1})} + {}^{z}A^{TM}_{j})]e^{+u_o z}\} J_1(\lambda r)d\lambda \quad , \quad \text{(A-66f)} $$

along with

$$ {}^{s}Y^{H}_{1o} = \int_0^\infty \{[{}^{-}B^{TM}_{oj}(e^{-u_j(z'-d_{j-1})} + {}^{x}A^{TM}_{j}) - \frac{\hat{z}_j u_o}{\hat{z}_o u_j} {}^{-}B^{TE}_{oj}(e^{-u_j(z'-d_{j-1})} + {}^{x}A^{TE}_{j})]e^{+u_o z}\} J_1(\lambda r)d\lambda \quad , \quad \text{(A-67a)} $$

$$ {}^{s}Y^{H}_{2o} = \int_0^\infty \{[{}^{-}B^{TM}_{oj}(e^{-u_j(z'-d_{j-1})} + {}^{x}A^{TM}_{j}) - \frac{\hat{z}_j u_o}{\hat{z}_o u_j} {}^{-}B^{TE}_{oj}(e^{-u_j(z'-d_{j-1})} + {}^{x}A^{TE}_{j})]e^{+u_o z}\} \lambda J_o(\lambda r)d\lambda \quad , \quad \text{(A-67b)} $$

$$ {}^{s}Y^{H}_{3o} = \int_0^\infty \frac{\hat{z}_j u_o}{\hat{z}_o u_j} \{[{}^{-}B^{TE}_{oj}(e^{-u_j(z'-d_{j-1})} + {}^{x}A^{TE}_{j})]e^{+u_o z}\} \lambda J_o(\lambda r)d\lambda \quad , \quad \text{(A-67c)} $$

$$ {}^{s}Y^{H}_{4o} = \int_0^\infty \frac{\hat{z}_j u_o}{\hat{z}_o u_j} \{[{}^{-}B^{TE}_{oj}(e^{-u_j(z'-d_{j-1})} + {}^{x}A^{TE}_{j})]e^{+u_o z}\} J_1(\lambda r)d\lambda \quad \text{(A-67d)} $$

and

$$ {}^{s}Y^{H}_{5o} = \int_0^\infty \frac{\lambda^2}{u_j} \{[{}^{-}B^{TM}_{oj}(e^{-u_j(z'-d_{j-1})} + {}^{z}A^{TM}_{j})]e^{+u_o z}\} J_1(\lambda r)d\lambda \quad , \quad \text{(A-67e)} $$

where ${}^{-}B^{TM}_{oj} = [1 + {}^{-}R^{TM}_{1}]\,{}^{-}B^{TM}_{1j}$ and ${}^{-}B^{TE}_{oj} = [1 + {}^{-}R^{TE}_{1}]\,{}^{-}B^{TE}_{1j}$.

APPENDIX B

PLANE WAVE FIELDS IN A LAYERED EARTH

For a vertically downward propagating incident plane wave at the surface, the general solution for the electric field in layer l is

$$\vec{E}_l(z) = \vec{E}_l^+ [e^{-ik_l(z-d_l)} + R_l e^{+ik_l(z-d_l)}] \quad , \quad \text{(B-1)}$$

with

$$\vec{E}_o(z) = \vec{E}_o^+ [e^{-ik_o z} + R_o e^{+ik_o z}] \quad \text{(B-2)}$$

in the air and

$$\vec{E}_n(z) = \vec{E}_n^+ e^{-ik_n(z-d_{n-1})} \quad \text{(B-3)}$$

in the basal half-space. The reflection coefficient relating upward and downward wave amplitudes at the bottom of the l layer is (Ward, 1967, p. 117)

$$R_l = \frac{\hat{Z}_{l+1} - Z_l}{\hat{Z}_{l+1} + Z_l} \quad , \quad \text{(B-4)}$$

in which $Z_l = \omega\mu_l/k_l$ and, with carat denoting apparent,

$$\hat{Z}_l = Z_l \frac{\hat{Z}_{l+1} + Z_l \tanh(ik_l h_l)}{Z_l + \hat{Z}_{l+1} \tanh(ik_l h_l)} \quad . \quad \text{(B-5)}$$

The thickness of the lth layer is h_l.

At the earth's surface,

$$\vec{E}_o(0) = \vec{E}_o^+ [(1.,0.) + R_o] \quad . \quad \text{(B-6)}$$

Since tangential $\vec{E}$-fields are continuous across interfaces, we find

$$\vec{E}_1(0) = \vec{E}_1^+[e^{+ik_1d_1} + R_1 e^{-ik_1d_1}] = \vec{E}_o(0) \quad , \quad \text{(B-7)}$$

so that

$$\vec{E}_1^+ = \vec{E}_o^+[(1.,0.) + R_o]e^{-ik_1h_1}/[(1.,0.) + R_1e^{-2ik_1h_1}] \quad , \quad \text{(B-8)}$$

where we have replaced d_1 by h_1. By induction,

$$\vec{E}_l^+ = \vec{E}_{l-1}^+[(1.,0.) + R_{l-1}]e^{-ik_lh_l}/[(1.,0.) + R_le^{-2ik_lh_l}] \quad \text{(B-10)}$$

and

$$\vec{E}_n^+ = \vec{E}_{n-1}^+[(1.,0.) + R_{n-1}] \quad . \quad \text{(B-11)}$$

In our algorithm, we set $\vec{E}_0^+ = (1.,0.)$ by convention.

From Maxwell's equations, the magnetic fields are

$$\vec{H}_l(z) = \frac{\omega\mu_l}{k_l}(\hat{k} \times \vec{E}_l^+)[e^{-ik_l(z-d_l)} - R_l e^{+ik_l(z-d_l)}] \quad \text{(B-12)}$$

and

$$\vec{H}_n(z) = \frac{\omega\mu_n}{k_n}(\hat{k} \times \vec{E}_n^+)e^{-ik_nz} \quad , \quad \text{(B-13)}$$

with $\hat{k}$ a unit vector in the z-direction.